POLISH MARITIME RESEARCH 2(82) 2014 Vol 21; pp. 9-26
10.2478/pomr-2014-0014

Resistance Prediction for Hard Chine Hulls in the Pre-Planing Regime

Dejan Radojcic[1)], Ph. D.,
Antonio Zgradic[2)], M. Sc.,
Milan Kalajdzic[1)], M. Sc.,
Aleksandar Simic[1], Ph. D.,
[1)] University of Belgrade, Belgrade, Serbia,
[2)] NAVAR, Herceg Novi, Montenegro

ABSTRACT

A mathematical representation of calm-water resistance for contemporary planing hull forms based on the USCG and TUNS Series is presented. Regression analysis and artificial neural network (ANN) techniques are used to establish, respectively, Simple and Complex mathematical models. For the Simple model, resistance is the dependent variable (actually R/Δ for standard displacement of Δ = 100000 lb), while the Froude number based on volume (F_{nV}) and slenderness ration ($L/V^{1/3}$) are the independent variables. In addition to these, Complex model's independent variables are the length beam ratio (L/B), the position of longitudinal centre of gravity (LCG/L) and the deadrise angle (β). The speed range corresponding to F_{nV} values between 0.6 and 3.5 is analyzed. The Simple model can be used in the concept design phases, while the Complex one might be used for various numerical towing tank performance predictions during all design phases, as appropriate.

Keywords: planing craft; hard chine hulls; resistance evaluation; Artificial-Neural-Network (ANN), TUNS Series, USCG Series; pre-planing regime

INTRODUCTION

Planing craft are by far the most common high speed marine vehicles that enable speeds considerably higher than those of displacement or semi-displacement type of vessels. Planing hulls have smaller resistance for speeds above F_{nL} = = 0.4, F_{nB} = 0.5 or F_{nV} = 1. For F_{nL}, F_{nB} and F_{nV} around 1, 1.5 and 3÷3.5 respectively, full planing is achieved when dominant hydrodynamic forces carry almost the whole weight of a vessel, while the buoyancy is relatively negligible. Note however that the vessel has to pass through three different regimes – displacement, semi-displacement and planing. To achieve this, the planing hull form, although simple, has certain peculiarities. Notably, it has pronounced hard chine (to enable flow separation), wide transom and straight stern buttock lines. Consequently, the planing hull-form and hull-loading parameters also differ from those used for conventional displacement vessels.

Planing craft resistance tests are rare, albeit needed, since misjudgements made in the early design phases may result in disappointing performance – something that is not so pronounced for the displacement vessels. Grouped calm-water resistance data obtained through the systematic model tests available in the public domain are:

a) Series EMB 50 and Russian Series BK and MBK – both obsolete
b) Series 62 (Clement and Blount 1963) together with its modifications for higher deadrise (Keuning et al 1982 and 1993) set the new standards in planing hull design
c) Series 65 was developed primarily for the hydrofoils, while recent Series SOTON (Taunton et al 2010) was mainly envisaged for higher speeds and comparison with the stepped hulls
d) Series TUNS (Delgado-Saldivar 1993) and USCG (Kowalyshyn and Metclaf 2006) – both appropriate for contemporary planing hulls.

Consequently, the data from the Series TUNS (Technical University of Nova Scotia) and USCG (United States Coast Guard) are used here to develop new mathematical models for resistance evaluation. The application zone for all planing hull series mentioned, as well as for the proposed mathematical model developed here, is shown in Fig. 1.

The calm-water resistance needed for power evaluation may be evaluated:

- directly from model tests (still regarded the most reliable)
- using Various mathematical models (usually based on the model tests)
- using Computational Fluid Dynamics – CFD, see for instance Savander et al (2010) and Garo et al (2012).

Since model tests are expensive, and CFD-based models are not yet sufficiently reliable or available for every day engineering applications, mathematical models are indispensable. Two main types of mathematical models are used:

- Regression Models – for instance Radojcic (1985 and 1991) and Keuning et al (1993) based on the Series 62 & 65 and 62 & 62 modified, respectively

- Empirical Models – amongst them Savitsky (1964) is by far the most frequently used.

The Savitsky model (initially derived for prismatic hulls only) was improved a few times (Savitsky 2006 and 2012, Blount and Fox 1976) and is mainly intended for pure planing regime, i.e. above $F_{nV} = 3$. The regression models, however, are used for a given hull form and in the speed range for which they have been derived.

A reliable mathematical model for resistance evaluations for the challenging speed range – the hump speeds – of up to $F_{nV} = 3$ or so, is clearly required. For higher speeds the Savitsky method seems to be reliable enough. Consequently, two speed-dependent math models are developed:

- Simple Model – developed through the application of regression analysis and based on only two dominant high-speed parameters, i.e. the slenderness ratio $L/V^{1/3}$ and F_{nV}, and
- Complex Model – developed through the application of Artificial Neural Network (ANN) and based on five principal high-speed parameters, i.e. the slenderness ratio $L/V^{1/3}$ and F_{nV}, but also the length beam ratio L/B, the position of longitudinal centre of gravity LCG/L and the deadrise angle β.

Both models are based on the contemporary planing hull forms, i.e. that of TUNS and USCG Series.

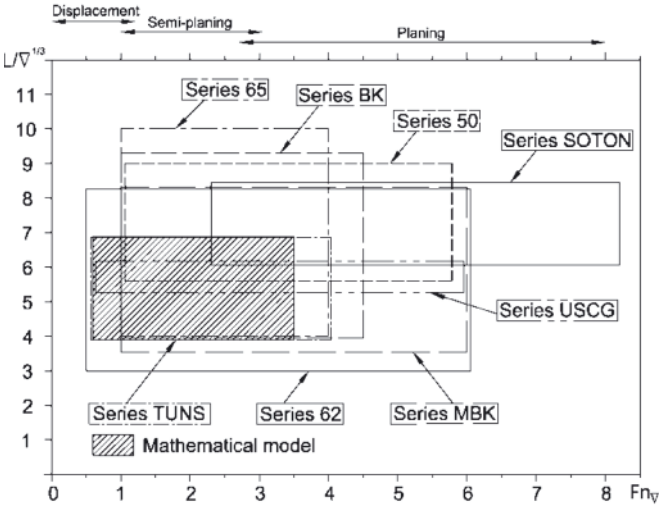

Fig. 1. *Planing-hull model resistance data available in public domain (adapted Schleicher and Bowles (2003) diagram)*

PLANING HULL PARAMETERS AND PERFORMANCE CHARACTERISTICS

The hull form and the loading characteristics are usually presented in dimensionless form and are the varied input parameters. The performance characteristics vary with speed, hence may be denoted as performance variables. The independent variables (or input parameters) are the hull form and the loading parameters, together with the dimensionless speed (Froude number). Note that the choice of appropriate planing-hull parameters that affect the performance is of utmost importance (see for instance Clement 1957, as the bases given there are still valid, also Blount 1993).

The principal challenge is the fact that the planing craft has to perform in (or through) three completely different regimes, i.e. displacement, semi-displacement and planing. Different hull-form and hull-loading parameters influence the performance in each of these regimes. For instance, according to Blount's discussion on the USCG Series (Kowalyshyn and Metclaf 2006), for F_{nV} values of 1.5, 2.5, 3.5 and 4.5, the resistance-to-weight ratio (R/Δ) depends mainly on:

For F_{nV}	R/Δ depends mainly on
1.5	the slenderness ratio ($L/V^{1/3}$)
2.5	both L/B and $L/V^{1/3}$
3.5	is almost independent of L/B and $L/V^{1/3}$
4.5	is dependent on L/B and $L/V^{1/3}$

Furthermore, considerations of hull-form and hull-loading parameters are not sufficient to produce the best mathematical model. Practicability and ready-availability of input data to a potential designer, at the initial design stages, should be considered as well. Bearing that in mind, the following hull-form and hull-loading parameters and performance variables were considered.

Hull form parameters

Ratio of length to beam is one of the hull form parameters that should obviously be used. According to Clement (1957) and the experience with the Series 62, it is obvious that the projected chine length L_p is better hull representative than other length measures (L_{WL} or L_{OA} for instance). L_p will be denoted as L from now on. The choice of Beam metric, however, is not so evident. In the past, the mean chine beam B_{PA}, the chine beam at transom B_{PT}, the maximum chine beam B_{PX}, the chine beam at LCG etc., were all used as effective beam metrics. Taking into account the hull form of TUNS and USCG series (B_{PX} is equal or almost equal to B_{PT}) B_{PX} is selected here, and is denoted just B. Consequently, $L_P/B_{PX} = L/B$.

Deadrise angle of hull bottom is also not standardized, as the representative β might be at $L_P/2$, i.e. $\beta_{Lp/2}$, at transom (β_T), midway $(\beta_{Lp/2}+\beta_T)/2$, at 70 % of L_P forward of transom (having Series 62 in mind), at LCG (β_{LCG}), at mean wetted length (having warped prismatic hull for the Savitsky method) etc. Here, the effective deadrise angle at B_{PX}, i.e. $\beta_{Bpx} = \beta$ is selected. Note that deadrise is not given in the dimensionless form.

Other hull form characteristics, such as the longitudinal curvature of the hull bottom (shape of buttock lines), the longitudinal distribution of chine beam, the type of sections etc. are all assumed to be similar to that of TUNS and USCG series, i.e. the mathematical model is valid for hull forms that are similar to those of TUNS and USCG models (see MacPherson 1996).

Hull loading parameters

Hull loading can be represented through the slenderness ratio – $L/V^{1/3}$, the planing area coefficient – $A_P/V^{2/3}$ or the beam-loading coefficient – V/B_{PX}^3 (used in the Savitsky method). The slenderness ratio was chosen to be the significant hull loading parameter, since the other two parameters are better for higher planing speeds.

Longitudinal Centre of Gravity LCG is modelled here through the ratio $LCG/L_P = LCG/L$ relative to the transom. LCG is often presented as the distance of the CG from the centroid of area A_P as percentage of L_P.

Performance characteristics

Choice of an adequate dimensionless speed parameter – the Froude number – is also of primary importance. Three Froude numbers are normally used, i.e. those based on volume

– $F_{nV} = v/(g \cdot V^{1/3})^{1/2}$, on length – $F_{nL} = v/(g \cdot L)^{1/2}$ and on breadth – $F_{nB} = v/(g \cdot B_{PX})^{1/2}$ (speed coefficient C_v for Savitsky method). F_{nL} and F_{nB} are good for low-displacement and high-planing speeds respectively (see Blount 1993, for instance). Given the speed range of interest here, and that the displacement is a fundamental design quantity (hence figures also in $L/V^{1/3}$, R/Δ and $S/V^{2/3}$), the volume Froude number F_{nV} is selected here for all further analyses.

Evaluation of full-scale calm-water resistance at certain speeds is a key objective of vessel design. To enable further analysis, the resistance data of both series were recalculated and transferred to the non-dimensional form R/Δ, for the high-speed-craft standard displacement of 100000 lb or 45.36 t, i.e. R/Δ_{100000}, is used – from now on just R/Δ.

This enables comparison of different hull forms. Moreover, in practice, a comparison is easier and more logical than the use of some other non-dimensional metric of merit (C_T for instance). A disadvantage, however, is that R/Δ has to be corrected for the displacements other than 100000 lb. Since:

$$R/\Delta = R/\Delta_{100000} + f\,(S/V^{2/3}, L_K/L)$$

the wetted area and the length of wetted area have to be available. Hence mathematical models for these parameters are also necessary. A design procedure, when R/Δ_{100000} is known, is not uncommon, and appropriate procedures can be found elsewhere.

The wetted area is usually presented in the non-dimensional form as $S/V^{2/3}$. However, the length of wetted area, needed for Reynolds number evaluation, is more debatable. Namely, for planing hulls R_n is usually evaluated by using the mean value of the lengths of wetted area at chine (L_C) and keel (L_K). For USCG Series, however, only L_K is used. It was therefore decided to use L_K throughout this work as the representative length of wetted surface for both TUNS and USCG series.

The use of L_K without deeper analysis (proof that L_K suffice) is justified by the fact that the spread of R/Δ values for displacements other than 100000 lb is relatively small. Therefore it is not necessary to determine $S/V^{2/3}$ and L_K/L with great accuracy. For instance, if both $S/V^{2/3}$ and L_K/L are wrongly defined (by even 30 %) maximal errors of R/Δ_{200000} and R/Δ_{10000} would be only around 1 % and 4 % respectively. If $S/V^{2/3}$ and L_K/L would be erroneously estimated by 10 %, which is much more likely, then errors of R/Δ_{200000} and R/Δ_{10000} would be around 0.4% and 1.3 % respectively. These errors are acceptable in this type of models.

Finally chosen parameters and performance variables – recapitulation

For analyses of TUNS and USCG series, as well as for the development of mathematical models for resistance evaluation (the wetted area and the length of wetted area), the following parameters and variables are chosen:

- Hull form and loading parameters: **$L/V^{1/3}$**, **L/B**, **LCG/L** and **β** (here $L = L_P$, $B = B_{PX}$, $\beta = \beta_{BPX}$).
- Performance characteristics: **F_{nV}** , **R/Δ**, **$S/V^{2/3}$** and **L_K/L** (here $\Delta = V \cdot \rho$, $L = L_P$, $R/\Delta = R/\Delta_{100000}$).

TUNS AND USCG SERIES

The goal is to extend the applicability of the well known USCG Series consisting of only 4 models, with much broader but less well known TUNS Series consisting of 9 models. In a way, these two similar series should form a new series that would be applicable to contemporary planing hull forms. A similar approach was used in Hubble (1974) and Radojcic (1985). The database of this new series is a starting point for establishment of the mathematical models for resistance evaluation. The database, and hence the subsequent mathematical models, are applicable for the displacement of 100000 lb in the sea water $\rho = 1026$ kg/m^3, temperature 15°C, viscosity $\nu = 1.1907 \cdot 10^{-6}$ m^2/s and ITTC-1957 friction coefficients with $C_A = 0$.

Note however that although the hull shape of both series is relatively similar, the facilities where the series were tested and accordingly the size of the models belonging to each series are completely different. Specifically, the USCG Series was tested in one of the world largest model basins, while the TUNS experiments were performed in a small university basin only 27 m long. Consequently, the USCG models were much larger, weighting between 135 and 220 kg, while the TUNS models weighted between 1 and 3.5 kg only. There is no doubt, therefore, which results are more reliable, and therefore all USCG data were weighted by a factor of 2. See Morabito and Snodgrass (2012) regarding the usefulness of small models, which may be the weakest point in this work.

More about each series can be found in original publications (Delgado-Saldivar 1993 and Kowalyshyn & Metclaf 2006). Table 1 tabulates the ranges of hull form and loading parameters for both series.

Tab. 1. *Ranges of hull form and loading parameters*

Series	L/B	β	$L/V^{1/3}$	$A_P/V^{2/3}$	LCG/L	F_{nV}
USCG	3.3-4.6	18-21	5.2-6.1	4.8-9.1	0.37-0.41	0.6-6.0
TUNS	2.5-3.5	12-24	3.9-6.9	5.2-11.6	0.27-0.38	0.6-4.0

Typical (parent hull) lines plans are shown in Figs. 2 and 3 for the USCG and TUNS Series, respectively. Note that the stern (or after) part of the TUNS Series is prismatic, i.e. sections are identical having the same deadrise, while the USCG models have slight variation – bottom warp and variable deadrise. The USCG models have also B_{PT} slightly narrower than B_{PX}. These differences are considered to be negligible, and hence were not accounted for, enabling the formation of a seamless database together with the simpler TUNS Series.

Comparison of USCG and TUNS performance characteristics

A comparison of performance characteristics in the overlapping zone (i.e. for hull and loading parameters that are the same for TUNS and USCG models) follows. As expected the performance characteristics (in this case the dynamic trim τ and the resistance-to-weight ratio R/Δ) for both series

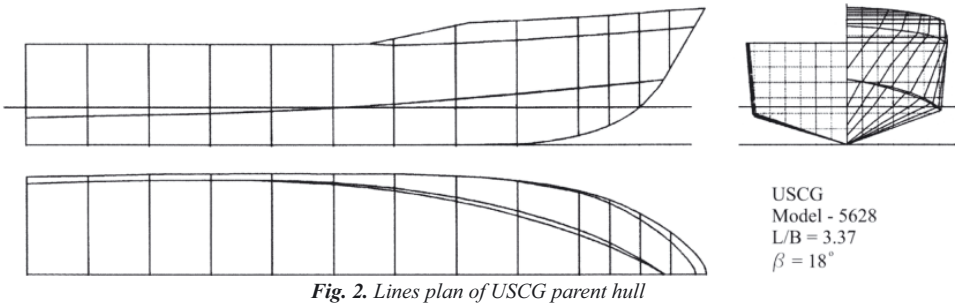

Fig. 2. *Lines plan of USCG parent hull*

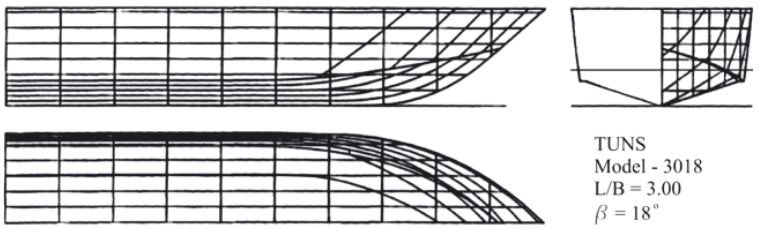

Fig. 3. *Lines plan of TUNS parent hull*

should be the same. Direct comparison of the performance characteristics is not possible since the models of each series had slightly different hull and loading parameters. Nevertheless, appropriate interpolations preformed within each series enable comparison. Typical results are shown in Figs. 4 and 5 for τ and R/Δ respectively.

In the overlapping zone, the τ values disagree to a great extent regardless of the kind of interpolation used. The R/Δ values, however, agree quite well. Generally, TUNS hump and below-hump values of R/Δ are slightly higher (than those of USCG). The depicted diagrams (and many more) are very convincing, so the development of a mathematical model for

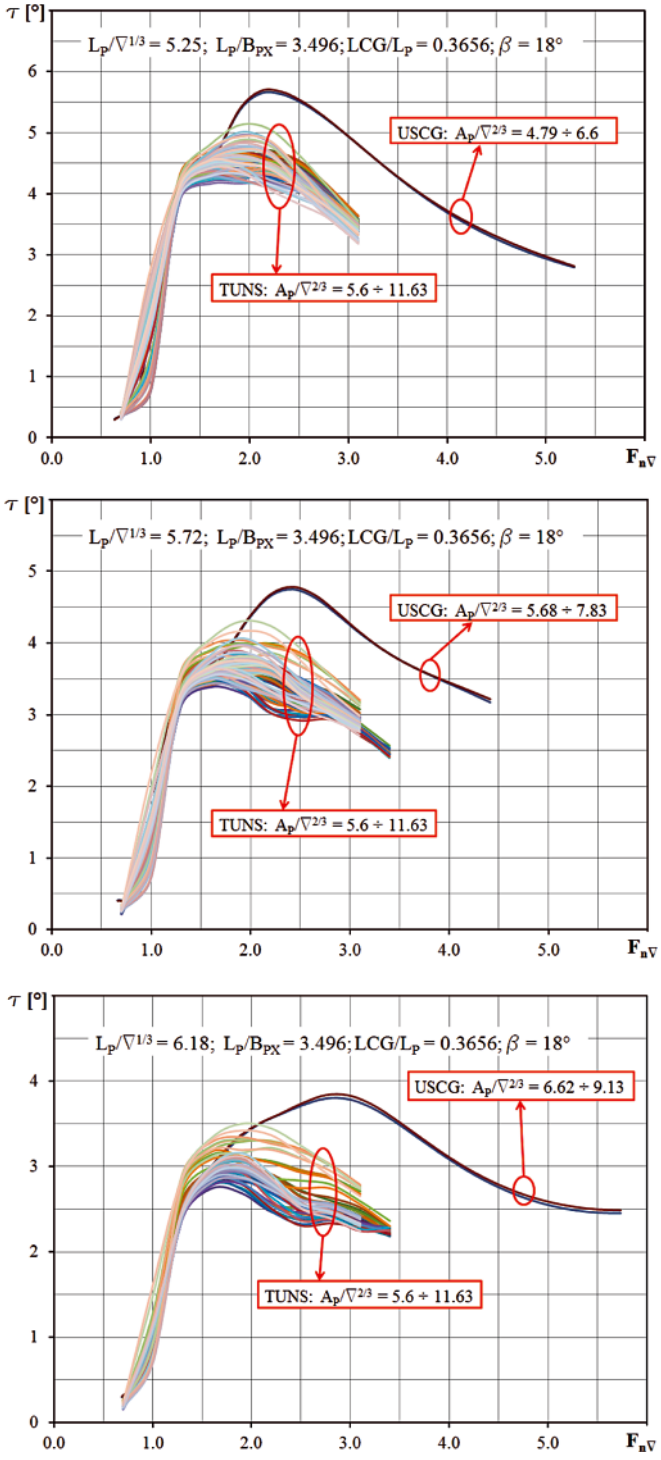

Fig. 4. *Typical τ values in the overlapping zone*

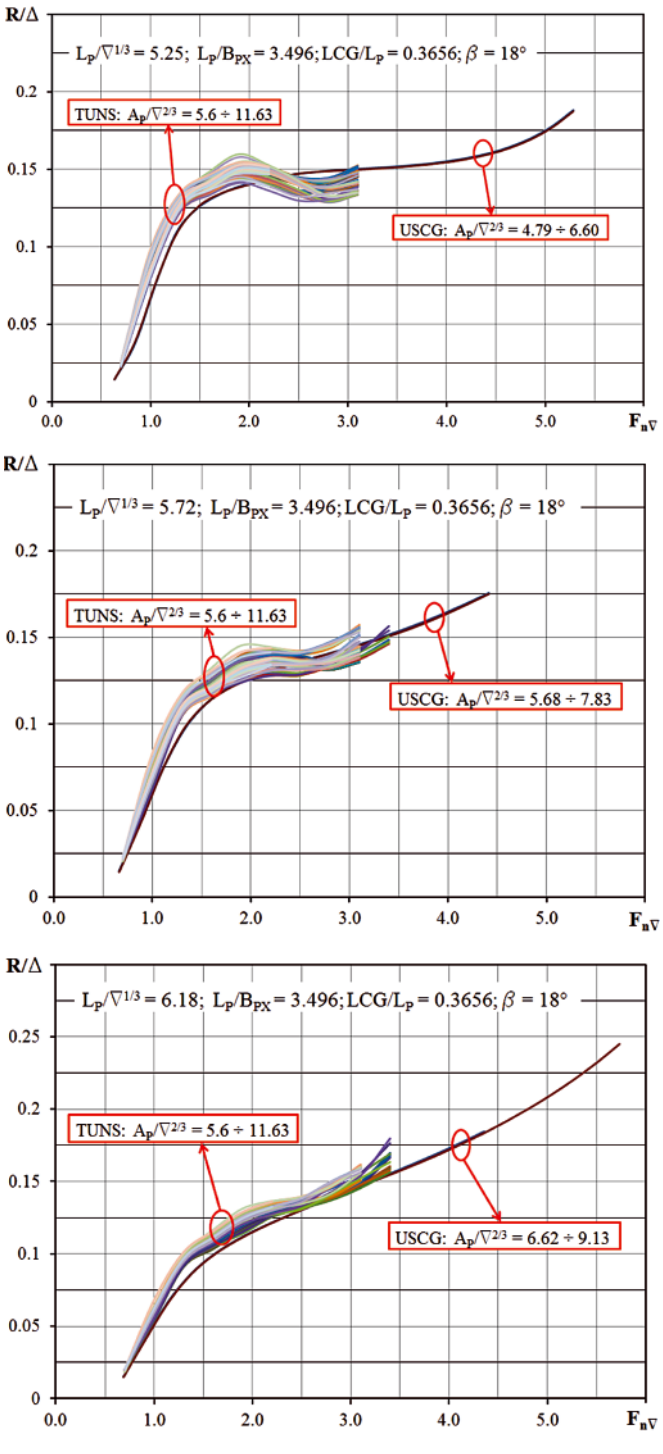

Fig. 5. *Typical R/W values in the overlapping zone*

evaluation of τ was abandoned, while the development of R/Δ mathematical model continued.

The τ values are obviously important, as τ and R/Δ mirror each other. This does not have to be the case with mathematical models based on model experiments. The Savitsky empirical model, mainly for planing speeds, is even dependent on τ. It should be noted that disagreements between τ_{TUNS} and τ_{USCG} seem to be systematic but rationalization of these disagreements, however, is beyond the scope of this paper.

Database for development of mathematical models for R/Δ evaluation

The database needed for the development of the mathematical model for R/Δ evaluation (for Δ = 100000 lb) can be generated on the conclusions reached so far. Few additional comments are needed:

- TUNS runs (data-points) which **a)** were incomplete (without $S/V^{2/3}$ and L_K), **b**) where porposing appeared or **c)** were obviously erroneous, were excluded from the database.
- For TUNS models the wetted length was calculated as $(L_K+L_C)/2$, while for the USCG models it was only L_K (L_C was not available).
- For the USCG models, the representative $\beta = \beta_{Bpx}$ was taken to be 18 and 21 degrees (at Station 7.5), and not 20 and 23 degrees (often stated values) which is at Station 6.
- For the USCG models L_P was estimated from the lines plan, while for the TUNS it was calculated as $L_P = L_{OA} \cdot 0.912$ (as suggested in the original Report).

All $R/\Delta = f(F_{nV})$ curves that were taken into account are shown in Fig. 6. Note that the final F_{nV} range is narrower and is between 0.6 and 3.5.

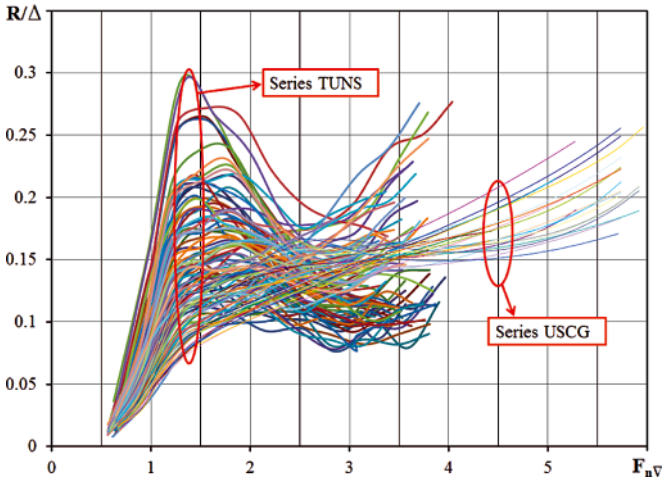

Fig. 6. $R/\Delta = f(F_{nV})$ curves taken into account for forming the database

ON APPLICATION OF ARTIFICIAL NEURAL NETWORK AND REGRESSION ANALYSIS

Two methods for development of mathematical models for resistance (R/Δ) evaluation were applied:

- Regression analysis for development of a Simple mathematical model and
- Artificial Neural Networks (ANN) for development of a Complex model.

In this section these two methods will be briefly compared from the mathematical model-maker's viewpoint.

When the regression analysis is applied, the independent variables consist of two sets of input data: a) Basic independent variables (hull parameters in this case), and b) Various powers and cross-products of powers of basic independent variables. Hence the initial polynomial equation can easily have 100 or more terms, although the number of basic parameters are usually around 5. If some hull's characteristic is not represented directly through the basic hull parameters, it will be represented indirectly through one of many polynomial terms that appear in the initial equation. Then, by applying a step-by-step procedure and statistical analysis, a best subset is chosen and less significant variables are rejected, ending with finally adopted equation which has considerably less independent variables; of the order of 10 to 20.

In contrast to the regression analysis, with the ANN method, more attention is paid to selection of independent variables. Specifically, the independent variables should be carefully chosen at the very beginning, because the final model will be based on the selected input parameters which form the input layers (X_k) for ANN. Incorrectly selected independent variables could result in an erroneous mathematical model, i.e. dependent variable (R/Δ) may be insensitive to the variations of a wrongly selected input variable. On the other hand, if a larger than necessary number of independent variables is assumed, validation of model stability becomes considerably more complex.

The artificial neural network which is used here (Rojas 1996, Miljkovic 2003, Zurek 2007) is of a feed-forward type with a back-propagation algorithm. The network can be expanded up to eight layers. Three types of activation functions, in which data are processed within the neurons, could be chosen: linear function, sigmoid function and hyperbolic tangent function. Sigmoid and hyperbolic tangent functions were thoroughly tested and the sigmoid function ($sig = 1/1 + e^{-x}$) was finally adopted since it produced better results. Both, the number of activation functions (3) and the number of layers (8), are limitations of the program that was used – aNETka 2.0 (see Zurek 2007).

Selection of the number of layers and number of neurons within each layer is very important, since when the equation becomes too complex instability might occur. Once the network configuration is adopted, the number of polynomial terms of a model can be pre-determined from the following expression (Simic 2012):

$$bc = \sum_{i}^{N-1}[(a_i + 1)\cdot a_{i+1}] + 2(a_1 + a_N)$$

where N represents the number of layers in the network and a_i is the number of neurons in each layer. So, for the mathematical model used here for evaluation of R/Δ (see below), the network is composed of five layers with configuration 5-7-5-3-1 (see Fig. 7), and the number of polynomial terms is:

$$\begin{aligned} bc &= [(a_1 + 1)\cdot a_2] + [(a_2 + 1)\cdot a_3] + [(a_3 + 1)\cdot a_4] + \\ &+ [(a_4 + 1)\cdot a_5] + 2(a_1 + a_5) = [(5 + 1)\cdot 7] + \\ &+ [(7 + 1)\cdot 5] + [(5 + 1)\cdot 3] + \\ &+ [(3 + 1)\cdot 1] + 2(5 + 1) = 116 \end{aligned}$$

Obviously, in order to find a 'good' solution, whether assessed in terms of accuracy, reliability or applicability, the number of layers and number of neurons in each layer has to be chosen by the model-maker in advance.

It should be noted that it is common practice to omit from the database the data that is intended to be used for verification of the reliability of the network. Consistent with the prior experience (for instance Simic 2012), the entire database was used for training of the algorithm, but considerable effort was invested in checking the reliability and stability of the derived mathematical model.

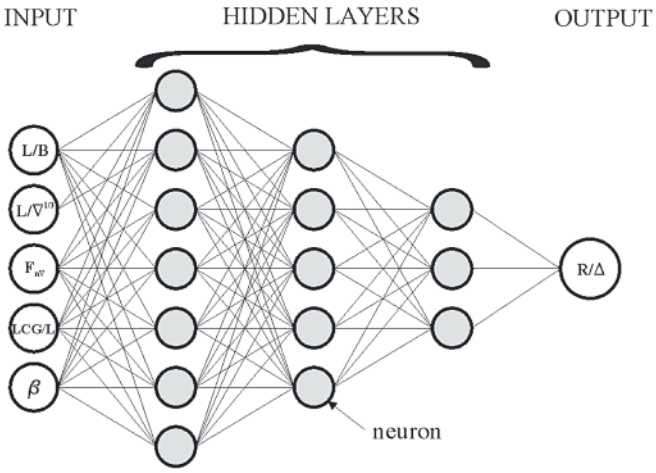

Fig. 7. ANN structure of finally adopted R/Δ mathematical model (configuration 5-7-5-3-1 with 3 hidden layers)

MATHEMATICAL MODELS

Simple mathematical model for R/Δ evaluation

The objective is to plot $R/\Delta = f(L/V^{1/3}, F_{nV})$ relationship, based on TUNS and USCG data, and to compare this with the well known diagram based on the Series 62 and 65, published in Hubble (1974), see Figure 8.

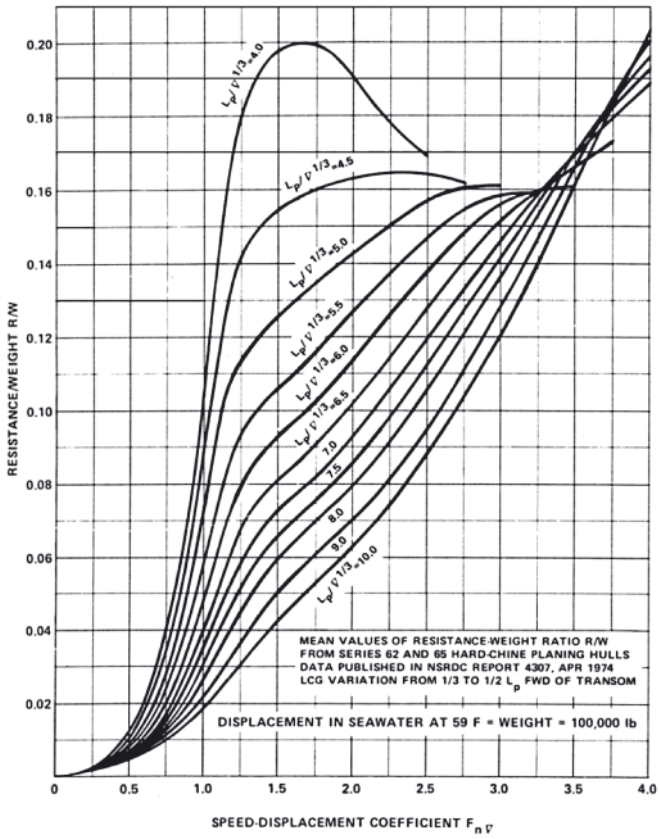

Fig. 8. Mean values of R/Δ from Series 62 and 65 data (Hubble, 1974)

This was done using the regression analysis options in Microsoft's Excel. The procedure, also used in Radojcic (1997), is the following:

a) Speed-dependent equations (with the same variables for all slenderness ratios) are developed first. Namely, the data having the same $L/V^{1/3}$ were grouped, regardless of the other hull form and loading parameters. 16 groups were formed. Then a trend line $R/\Delta = f(F_{nV})$ was produced (a cubic parabola $y = A \cdot x^3 + B \cdot x^2 + C \cdot x + D$) for each group. Figure 9 shows the results for $L/V^{1/3} = 3.90$; 5.46 and 6.87.

b) A second regression analysis is then performed with the regression coefficients cross-faired against the slenderness ratio. So, four new diagrams are then formed, one for each coefficient, i.e. A, B, C, D = $f(L/V^{1/3})$. See Figure 10.

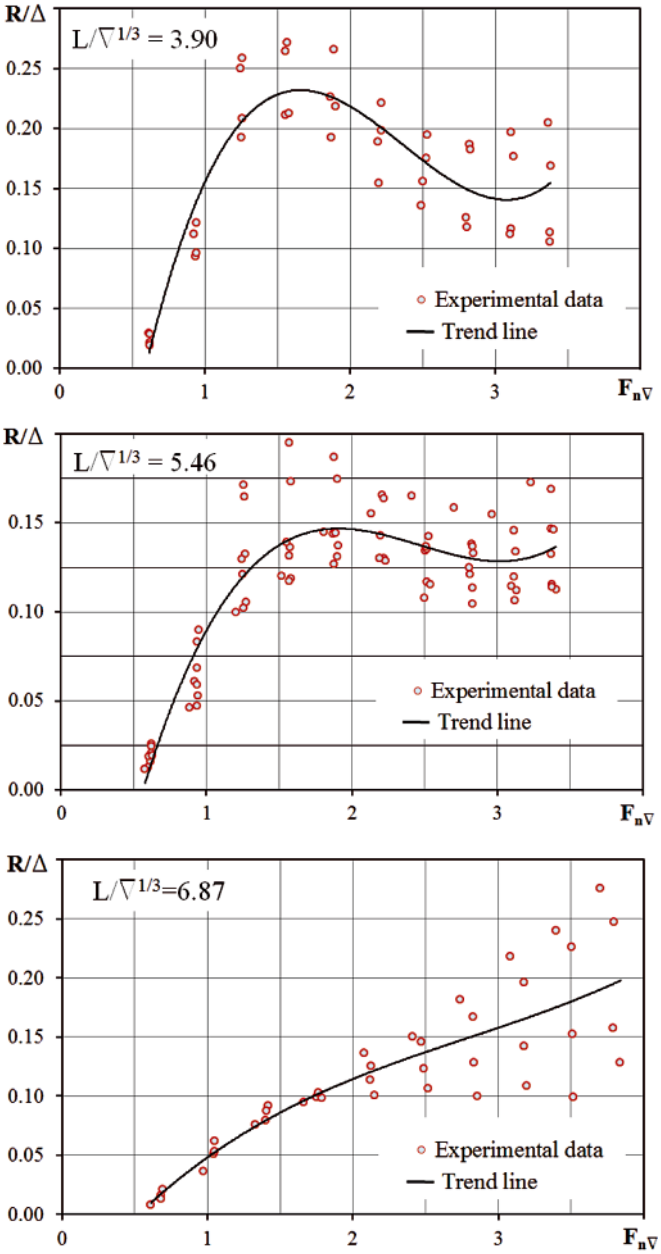

Fig. 9. $R/\Delta = f(F_{nV})$ for $L/V^{1/3} = 3.90$; 5.46 and 6.87

Thus, the first step develops speed dependent equations for discrete $L/V^{1/3}$ values. The second step extracts F_{nV} and $L/V^{1/3}$ dependent equations – represented as a surface $R/\Delta = A \cdot F_{nV}^3 + B \cdot F_{nV}^2 + C \cdot F_{nV} + D$, as shown in Figs. 11 and 12. The diagram in Fig. 11 is obviously comparable to the one in Fig. 8.

A similar procedure is repeated for $S/V^{2/3}$ and L_K/L – as needed for evaluation of R/Δ for displacements other than 100000 lb. See resulting Figs. 13 to 16.

Given the scattered initial data and coefficients, as shown in Figs. 9 and 10 respectively, it is amazing that exceptionally nice diagrams can be produced using a simple procedures available in Excel. Power of statistics and regression is also confirmed. Moreover, having the $R/\Delta = f(L/V^{1/3}, F_{nV})$ relationship is very useful, especially during the concept design phases when hull form parameters are typically unknown but the relation

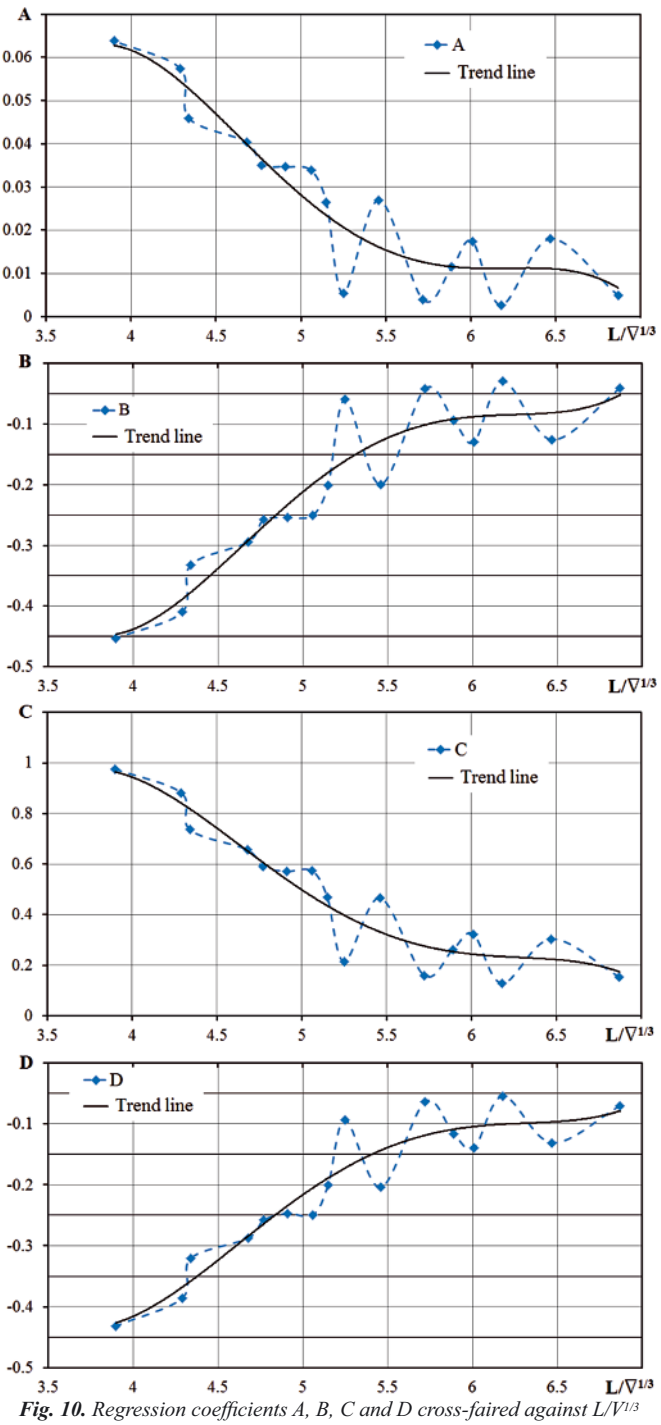

Fig. 10. Regression coefficients A, B, C and D cross-faired against $L/\nabla^{1/3}$

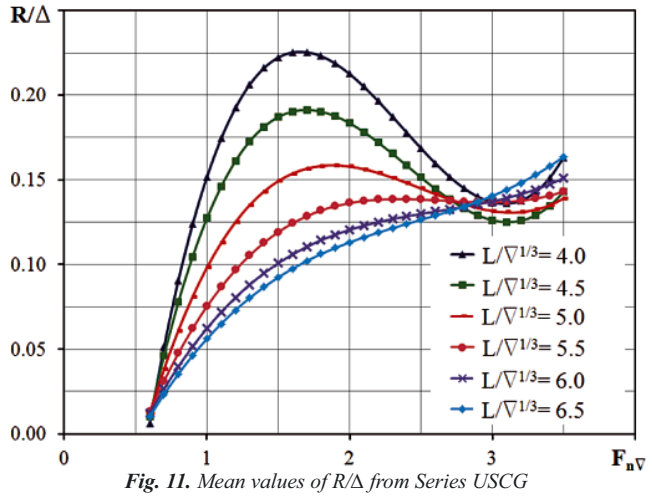

Fig. 11. Mean values of R/Δ from Series USCG and TUNS data – 2D diagram

between the vessel length and weight is desired. Nevertheless, users are reminded that the Simple model is a single parameter formulation and that resistance predictions are of reduced quality when hull parameter boundaries other than that of slenderness ratio are approached.

Coefficients A, B, C and D for evaluation of R/Δ, $S/V^{2/3}$ and L_K/L are given in Appendix 1.

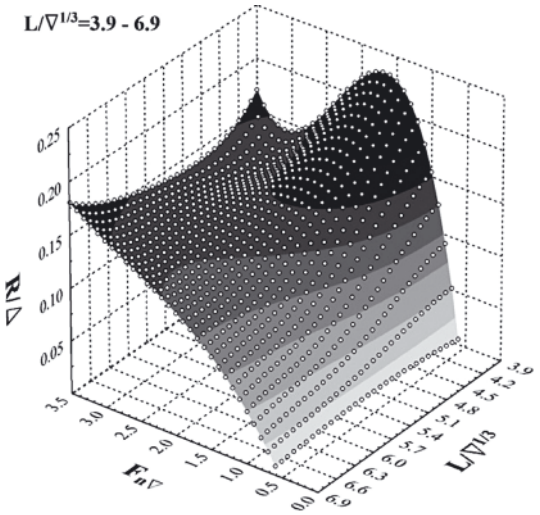

Fig. 12. Mean values of R/Δ from Series USCG and TUNS data – 3D diagram

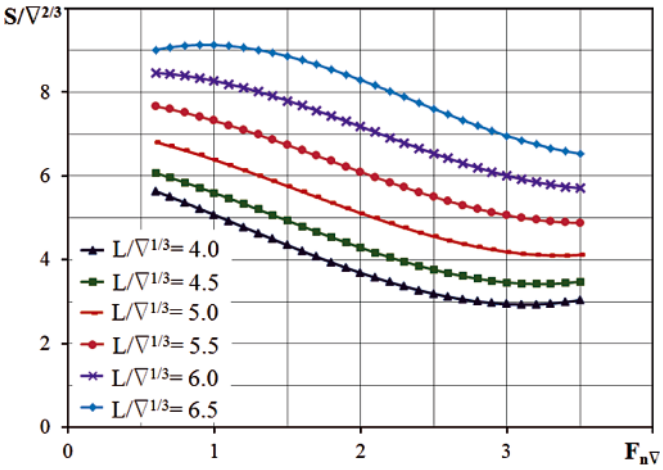

Fig. 13. Mean values of wetted area coefficient $S/V^{2/3}$ from Series USCG and TUNS data – 2D diagram

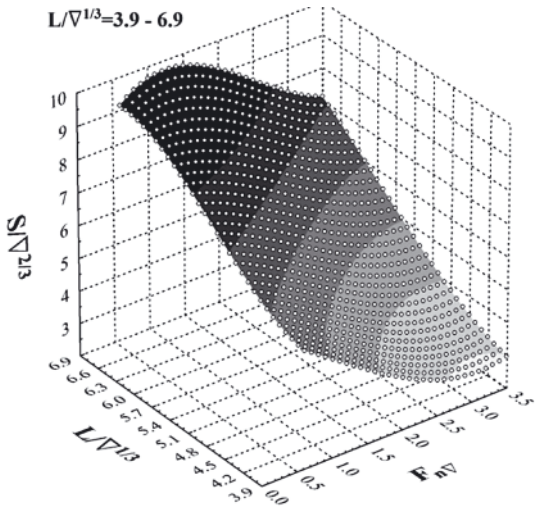

Fig. 14. Mean values of wetted area coefficient $S/V^{2/3}$ from Series USCG and TUNS data – 3D diagram

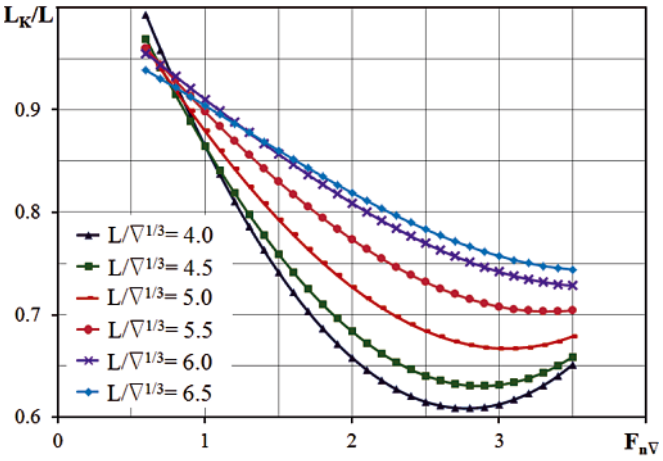

Fig. 15. *Mean values of length of wetted area L_K/L from Series USCG and TUNS data – 2D diagram*

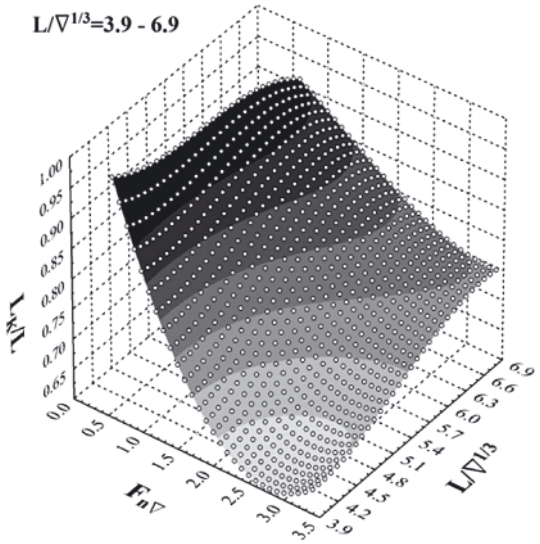

Fig. 16. *Mean values of length of wetted area L_K/L from Series USCG and TUNS data – 3D diagram*

Complex mathematical model for R/Δ evaluation

ANN possibilities, procedures etc. were explained in the previous section. This section explains the development of the Complex mathematical model (vs. the Simple Model previously explained) for the evaluation of:

- $R/\Delta = f(L/V^{1/3}, F_{nV}, L/B, LCG/L, \beta)$,
- $S/V^{2/3} = f(L/V^{1/3}, F_{nV}, L/B, LCG/L)$ and
- $L_K/L = f(F_{nV}, LCG/L)$.

The last two variables are obviously simpler, so the procedure for the R/Δ model is explained in more details, but the results for all three variables are given.

Several mathematical models for R/Δ were derived and tested, see Table 2. Considerable time was spent for stability checks of the derived models (oscillations in results for values between data points used for the mathematical model derivation). Several derived models with several hundred terms produced good results but were rejected as too complex and impractical for a user/designer. The finally adopted model with 116 polynomial terms follows:

$$Y = \frac{\mathrm{sig}\left(d_v + \sum_{w=1}^{3}\left(D_{wv} \times \mathrm{sig}\left(c_w + \sum_{i=1}^{5}\left(C_{iw} \times \mathrm{sig}\left(b_i + \sum_{j=1}^{7}\left(B_{ji} \times \mathrm{sig}\left(a_j + \sum_{k=1}^{5}\left(A_{kj} \times (P_k X_k + R_k)\right)\right)\right)\right)\right)\right)\right) - G}{H}$$

where:
$X_K = \{L/B, L/V^{1/3}, F_{nV}, LCG/L, \beta\}$
$Y = R/\Delta$
G, H, P_k, R_k, A_{kj}, B_{ji}, C_{iw}, D_{wv}, a_j, b_i, c_w, d_v are the coefficients.

Tab. 2. *Configurations of tested mathematical models for R/Δ evaluation*

No. of terms	No. of hidden layers	No. of considered M.M.	RMS*)	Fn_V
400 ÷ 750	4	30	2.6 ÷ 3.6	0.6 ÷ 6.0
200 ÷ 250	1 to 4, mainly 3	20	3.7 ÷ 5.3	0.6 ÷ 6.0
150 ÷ 200	1 to 4, mainly 3	29	4.2 ÷ 5.7	0.6 ÷ 6.0
80 ÷ 150	1 to 3, mainly 2	21	4.6 ÷ 5.9	0.6 ÷ 6.0
116	**3**	**Finally adopted M.M.**	**5.43**	**0.6 ÷ 6.0**

*) RMS - according to aNETka. Manually calculated RMS is slightly different.

Note that no additional screening of obviously wrong data was done even after the derivation of the final model which clearly highlighted outliers. If that step was introduced and a new math model was then derived, the RMS would be considerably lower. Nevertheless, the quality of that model would be just about the same as of one used here. The RMS value is actually irrelevant, and is used only for the comparison of various models based on a same database.

26 models were derived for the wetted area coefficient ($S/V^{2/3}$), and the one finally selected has 23 polynomial terms with RMS of around 10 %.

$$Y = \frac{\mathrm{sig}\left(b_i + \sum_{j=1}^{2}\left(B_{ji} \cdot \mathrm{sig}\left(a_j + \sum_{k=1}^{4}\left(A_{kj} \cdot (P_k X_k + R_k)\right)\right)\right)\right) - G}{H}$$

where:
$X_K = \{L/B, L/V^{1/3}, F_{nV}, LCG/L\}$
$Y = S/V^{2/3}$
G, H, P_k, R_k, A_{kj}, B_{ji}, a_j, b_i are the coefficients.

A simple speed-dependent relation was required for the length of wetted area (L_K/L). There was no need to use ANN, it was derived simply by the application of the regression analysis. The finally selected mathematical model has 16 polynomial terms with RMS of around 9 %.

$$\frac{L_K}{L} = A \cdot F_{n\nabla}^{\ 3} + B \cdot F_{n\nabla}^{\ 2} + C \cdot F_{n\nabla} + D$$

For all three equations, polynomial coefficients are given in Appendix 2. All three equations are approximately valid for the following range:

$$3.9 \le L/V^{1/3} \le 6.9$$
$$2.5 \le L/B \le 4.7$$
$$0.6 \le F_{nV} \le 3.5$$
$$0.27 \le LCG/L \le 0.41$$
$$12 \le \beta \le 24$$

The boundaries of applicability of the models are depicted in Fig. 17, while the boundaries suitable for programming are given in Appendix 2. The boundaries are actually the surfaces which bound the multidimensional space.

The boundaries of applicability (Fig. 17) require additional discussion. Note:

a) TUNS and USCG Zones are formed according to hull-form and loading parameters of each particular model (dots) that form the series. Shown is Overlapping Zone as well.
b) Unreliable Zone (seen on the $\beta = f(LCG/L)$ diagram only) is the zone where the mathematical model gives good results (the test data are well represented by the mathematical model) but the data is not logical, i.e.is most probably erroneous.
c) Rejected Zones (seen on the $\beta = f(LCG/L)$ and $L/B = f(LCG/L)$ diagrams) are the zones where the mathematical model is unstable (gives relatively bad results with saddles and humps for the interpolated values).
d) Lines denote the boundaries of applicability (borders) of the mathematical model (adjacent numbers indicate simple linear equations given in Appendix 2).

Discussion concerning complex mathematical model

The number of terms (116) in the polynomial seems large, but it should be noted that the Froude number is one

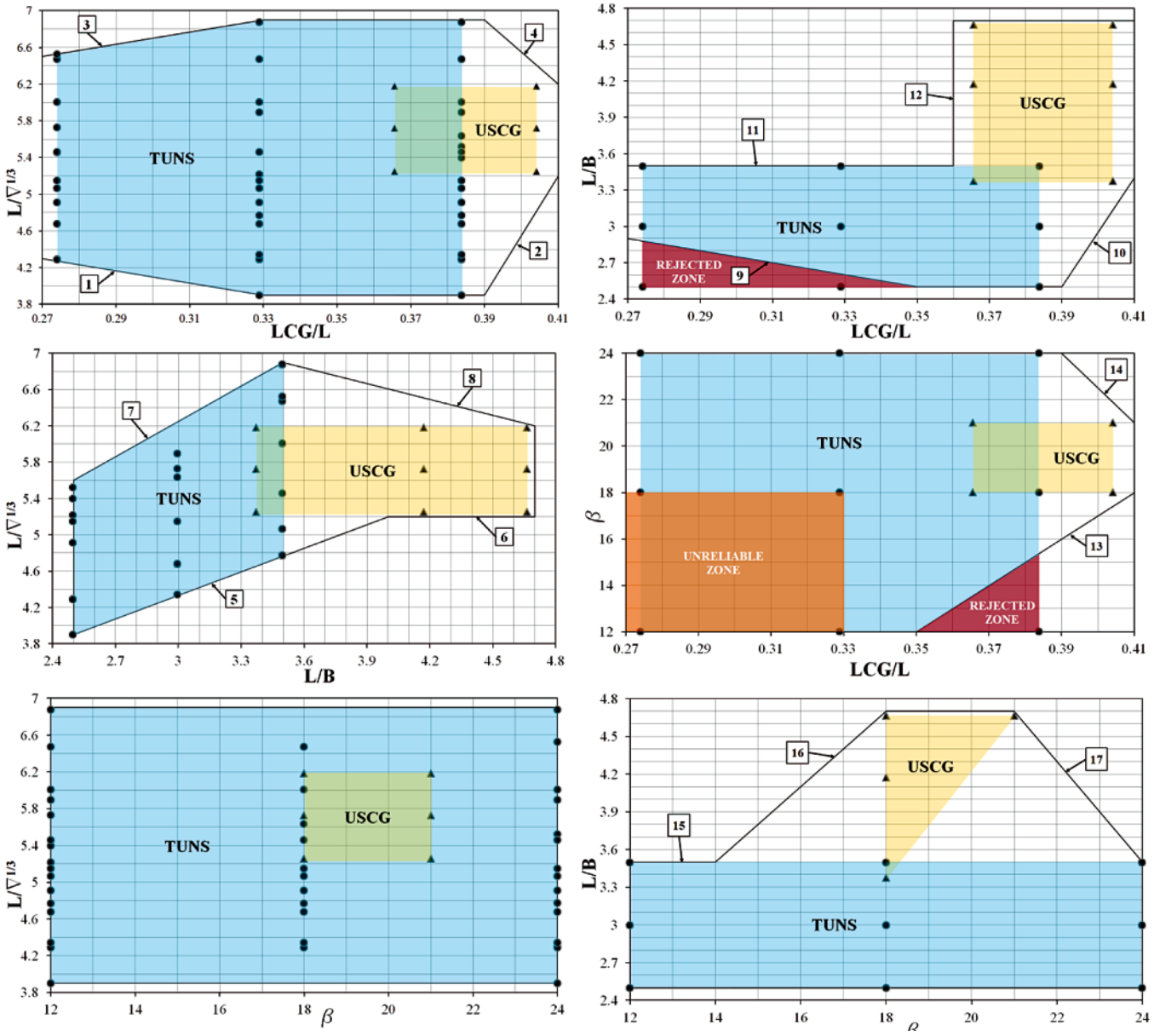

Fig. 17. Boundaries of mathematical model applicability (Boundaries suitable for programming are given in Appendix 2)

of independent variables. In comparable speed-independent mathematical models, for instance Radojcic (1991), R/Δ is evaluated for each Froude number separately, so for F_{nV} range of up to 3.5 around 120 terms were needed (around 15 for each equation). In Radojcic et al (1997) speed-independent and speed-dependant math models were derived, albeit for semi-displacement NPL Series, both having around 150 polynomial terms. A disadvantage of speed-independent models, although often more accurate for one speed, is that the resistance computed at one speed is not directly linked to that at another speed. So to obtain $R/\Delta = f(F_{nV})$ curve, smoothing is often necessary.

Note that both, Simple and Complex mathematical models for L_K/L, have the same number of polynomial terms and that the input variables – besides F_{nV} – are $L/V^{1/3}$ and LCG/L respectively, i.e. both model types depend on only two variables. Nevertheless, the second one is more accurate (RMS is 9 % vs. 16 %), confirming that LCG/L is more influential parameter for L_K evaluation than $L/V^{1/3}$.

More than a thousand 2D and 3D diagrams were constructed in order to check the quality of the derived mathematical model and the suggested boundaries of applicability. This facilitated examination of the 6-dimensional R/Δ surface from different angles. Some of typical diagrams deserve discussion. For instance, the diagrams depicted in Figs. 18 to 21 illustrate

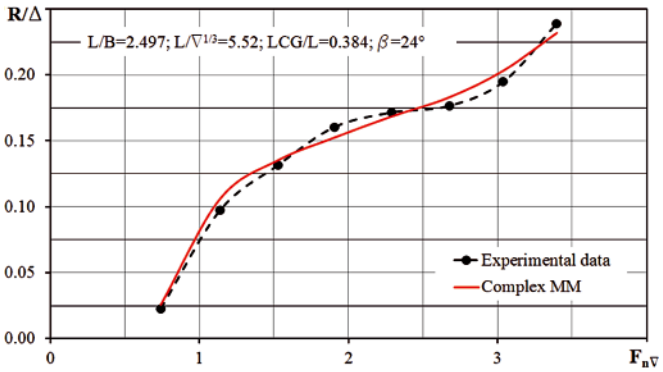

Fig. 18. R/Δ tested and evaluated on applicability boundaries

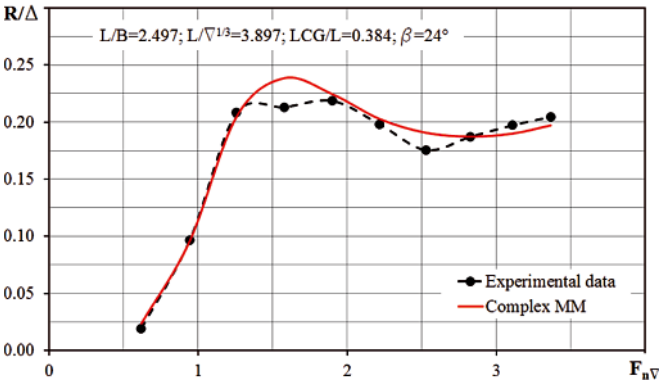

Fig. 19. R/Δ tested and evaluated on applicability boundaries

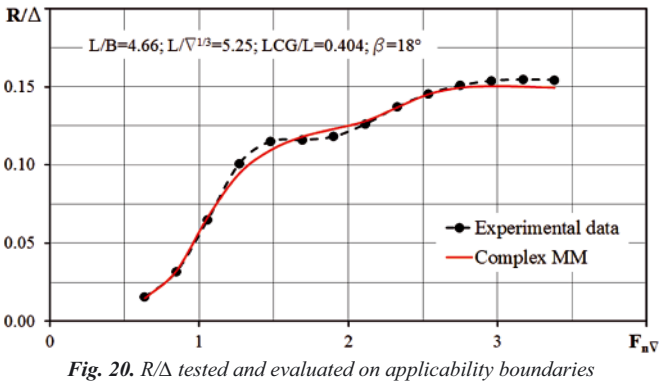

Fig. 20. R/Δ tested and evaluated on applicability boundaries

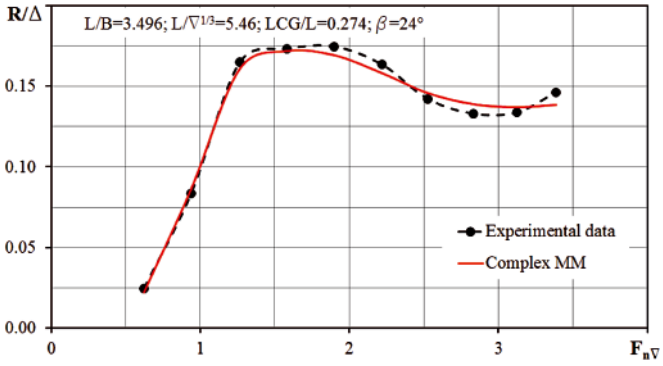

Fig. 21. R/Δ tested and evaluated on applicability boundaries

the correlation between the mathematical model and real experiments on the boundaries of applicability, where the match should be lower than in the middle of the applicability zone.

Discrepancies are obviously small. Moreover, it is almost certain that the mathematical model smoothed out some erroneous measurements, as for instance those in Fig. 19. In the same diagram, for instance, the discrepancies (measured to modelled) for F_{nV} values of 0.6, 1.6 and 3.4 are 23 %, 12 % and 4 % respectively.

Note that the reliability of some TUNS data is questionable. In some cases there were just a few erroneous points which could easily be disregarded. But in other cases there were complete measurement sets that were obviously erroneous and not logical; see for instance Fig. 22 (curve for β = 18 is below β = 12, which is impossible). Often the mathematical model followed those erroneous data-points, see Fig. 23 which is typical for the so called Unreliable Zone.

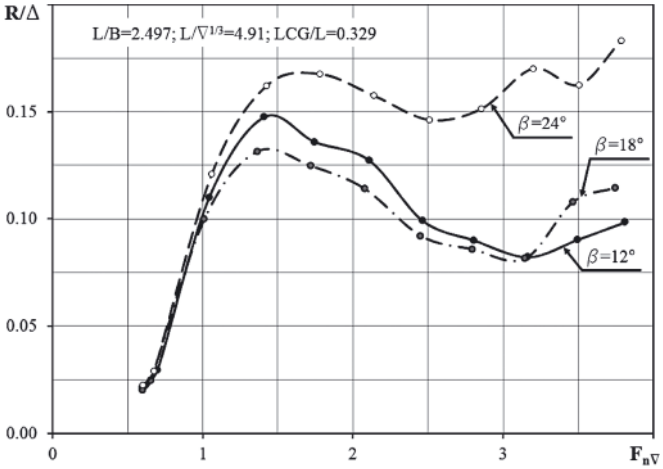

Fig. 22. Experimental R/Δ data for β = 12°, 18° and 24° in the unreliable zone

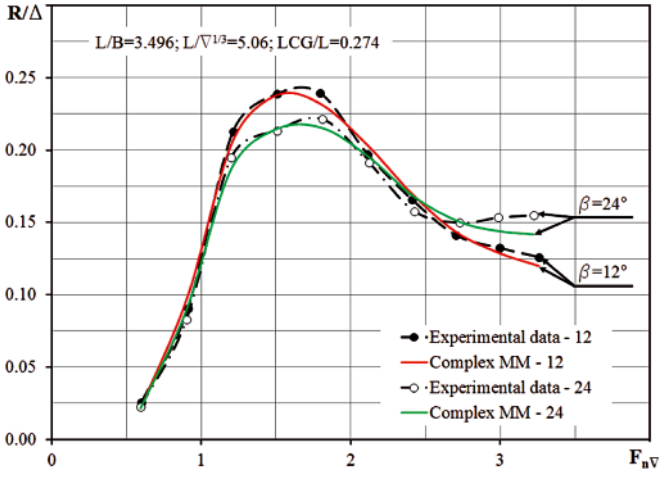

Fig. 23. R/Δ tested and evaluated in the unreliable zone

The reasons for the appearance of the Rejected Zone are typically depicted in the Fig. 24 where the saddle was avoided by reducing part of the applicability zone. Namely, the mathematical model unsatisfactorily followed the experimental data.

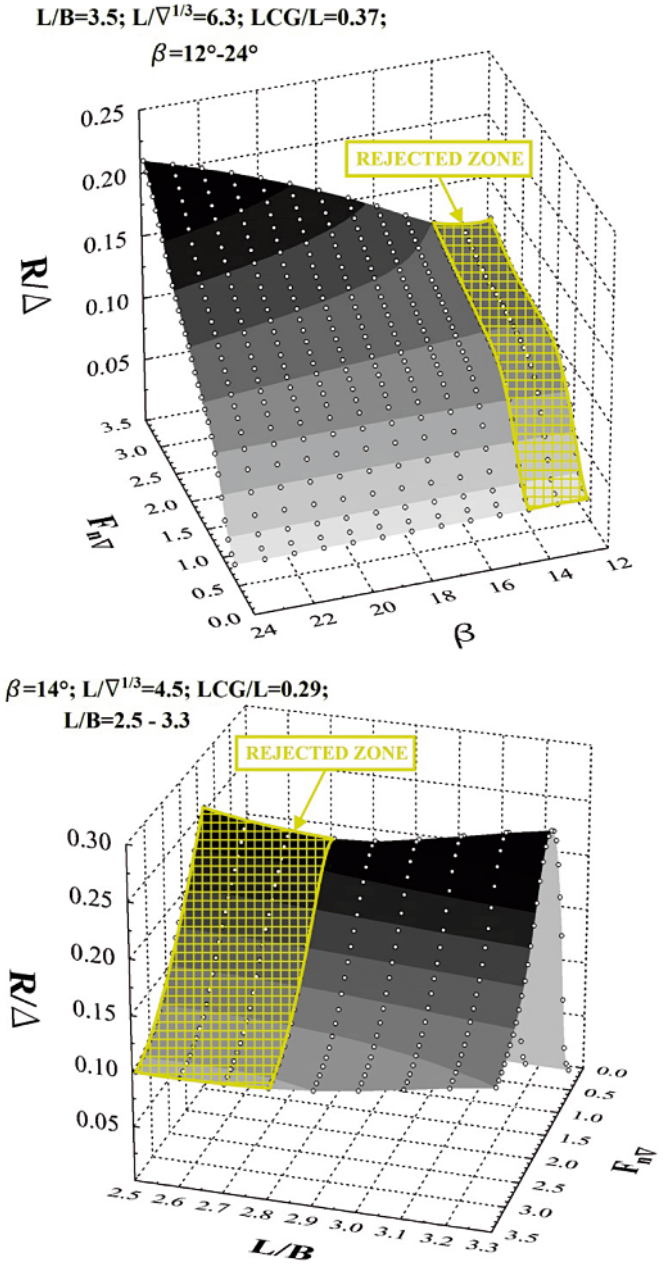

Fig. 24. Reduction of the applicability zone due to saddle

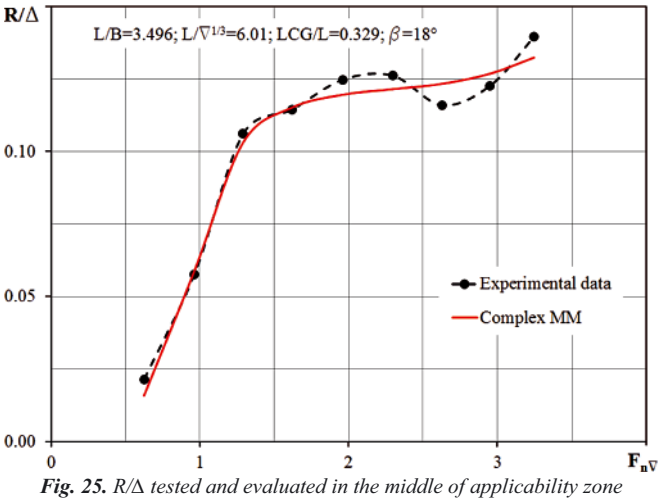

Fig. 25. R/Δ tested and evaluated in the middle of applicability zone

Figs. 25 and 26 depict the discrepancies in the middle of the applicability zone. As with the previous diagrams (Figs. 18-21 and 23), the agreement between the TUNS and USCG Series R/Δ values and those obtained by the mathematical model is fairly good. The mathematical model produced results that made more logical sense than the measurements due its inherent smoothing capabilities.

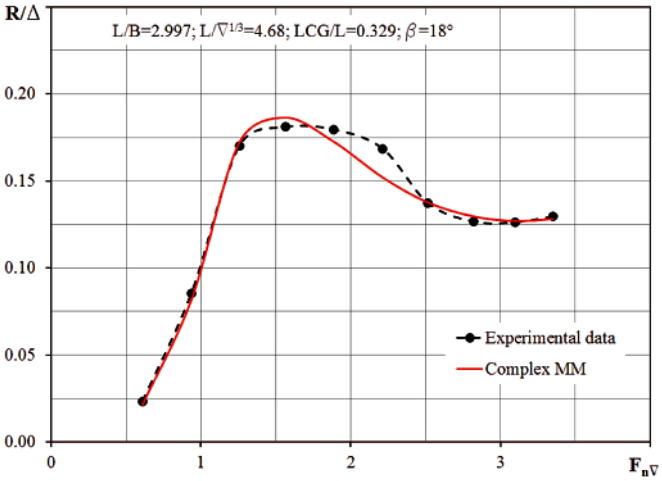

Fig. 26. R/Δ tested and evaluated in the middle of applicability zone

The quality of the derived mathematical model within the boundaries of applicability is described by 3D diagrams in Figs. 27 to 34. The presented cases are chosen ad hoc, with intention to provide the evidence that there were no instabilities in the model. So,

- Figs. 27 and 28 describe the influence of $L/V^{1/3}$ variation
- Figs. 29 and 30 describe the influence of LCG/L variation
- Figs. 31 and 32 describe the influence of β variation
- Figs. 33 and 34 describe the influence of L/B variation.

Note that the diagram in Fig. 34 looks a bit wavy, and hence needs additional examination as shown in Figs. 35 and 36. Namely, the 3D diagram shown in Fig. 35 has $L/V^{1/3} = 5.2$, which is close to $L/V^{1/3} = 5.5$ of the 3D diagram in Fig. 34 (all other parameters being the same). For $L/V^{1/3} = 5.2$, however, there are test data curves ($R/\Delta = f(F_{nV})$ of USCG models 5628, 5629 and 5630 with L/B = 3.37, 4.17 and 4.66 respectively. These are drawn on the surface evaluated by the mathematical model (see Figure 35).

Obviously, the discrepancies between the test-data (lines) and the mathematical model (surface) are small. This is illustrated better in Fig. 36. So, the mathematical model describes the USCG test data very well. The model test-data for R/Δ of TUNS Series, however, are slightly different (see Figure 5), and hence strongly influence the surface for L/B values below 3.37, resulting in a hollow for L/B above 2.5 and below 3.37. In other words, the merger between the TUNS and USCG Series is not seamless. This is unavoidable drawback when two series are merged to form a new series, actually a joint data-base.

Note that some future mathematical model may be more accurate and have slightly broader boundaries of applicability. But it cannot be expected that it would be much better, since mathematical models cannot be more accurate than the measurement data they are based on, and, as already stated, some of the baseline data is obviously erroneous. Ergo, derivation of better models requires better measured data. Note, however, that a few erroneous measurements do not compromise the validity of the entire TUNS Series.

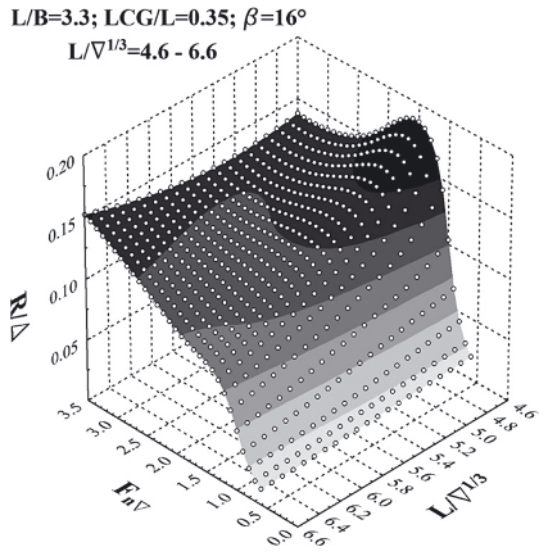

Fig. 27. The influence of $L/V^{1/3}$ on R/Δ

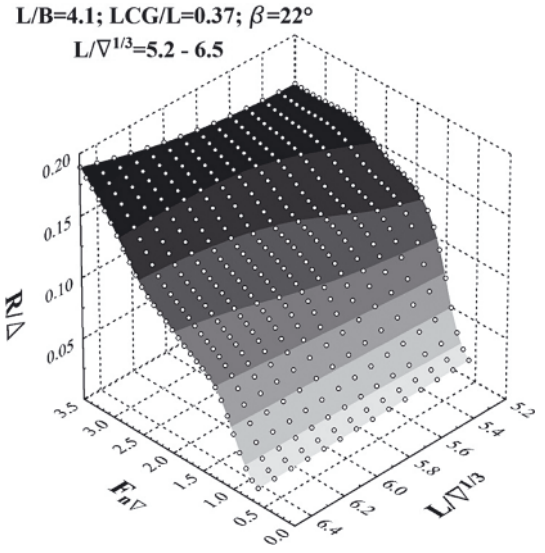

Fig. 28. The influence of $L/V^{1/3}$ on R/Δ

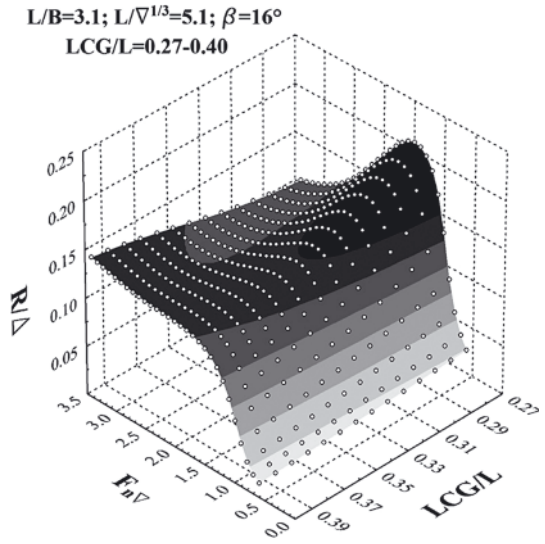

Fig. 30. The influence of LCG/L on R/Δ

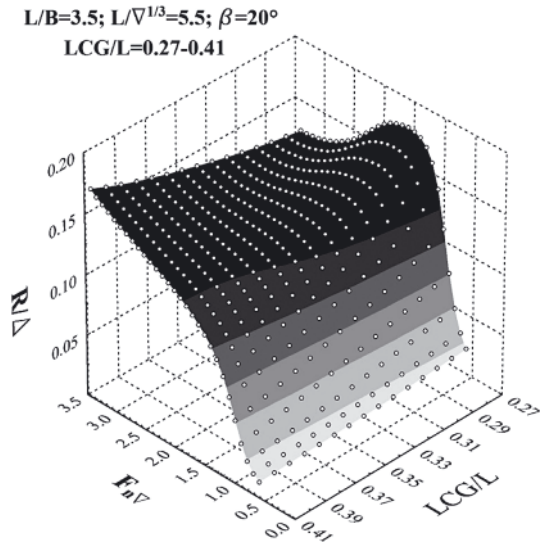

Fig. 29. The influence of LCG/L on R/Δ

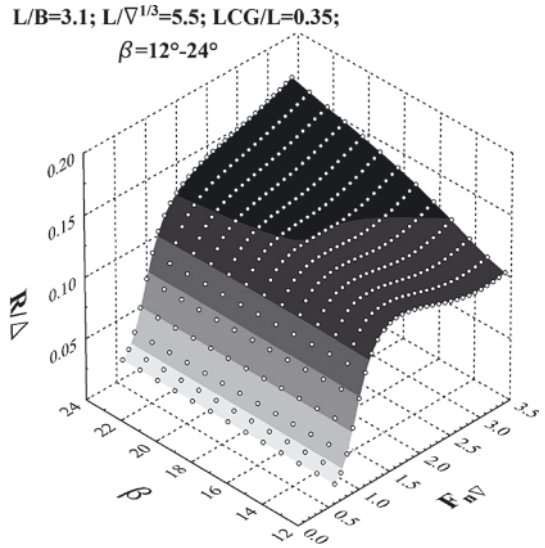

Fig. 31. The influence of β on R/Δ

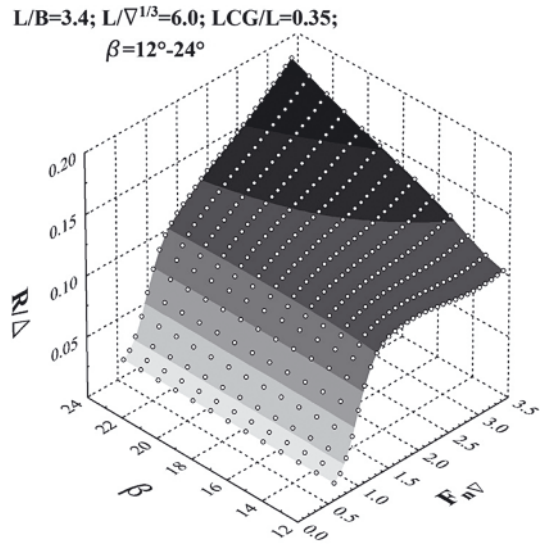

Fig. 32. The influence of β on R/Δ

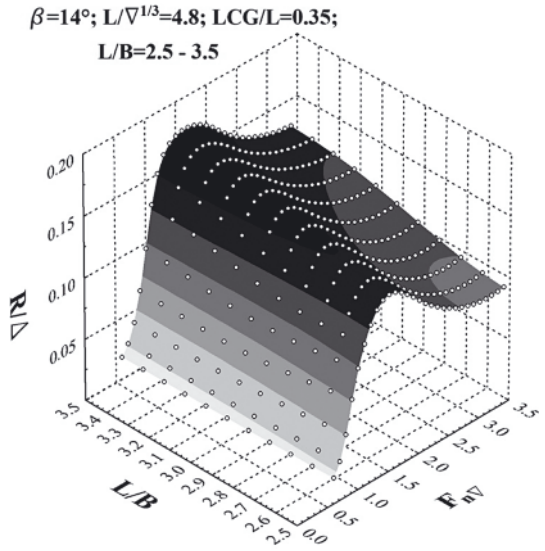

Fig. 33. The influence of L/B on R/Δ

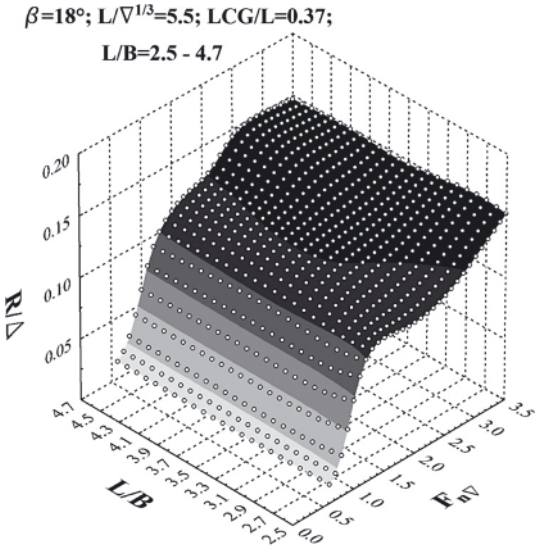

Fig. 34. The influence of L/B on R/Δ

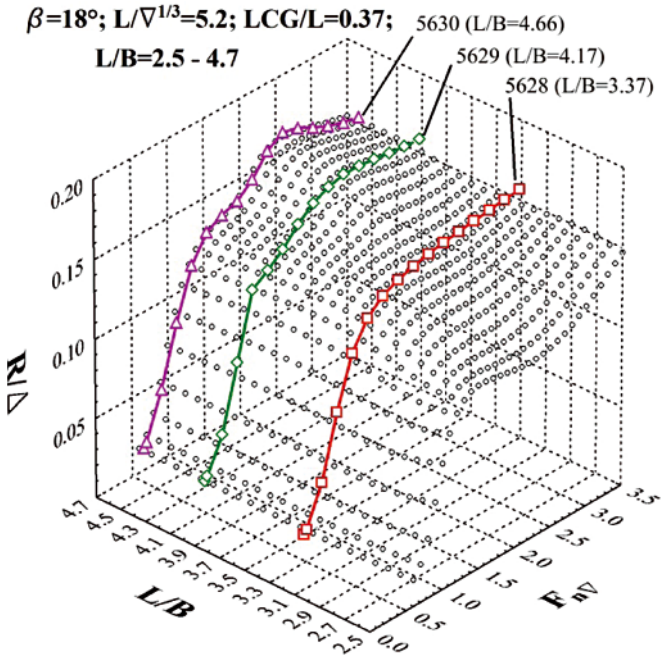

Fig. 35. R/Δ = f(F$_{n\nabla}$) curves of USCG models 5630, 5629 and 5628 drawn on the surface evaluated by the mathematical model

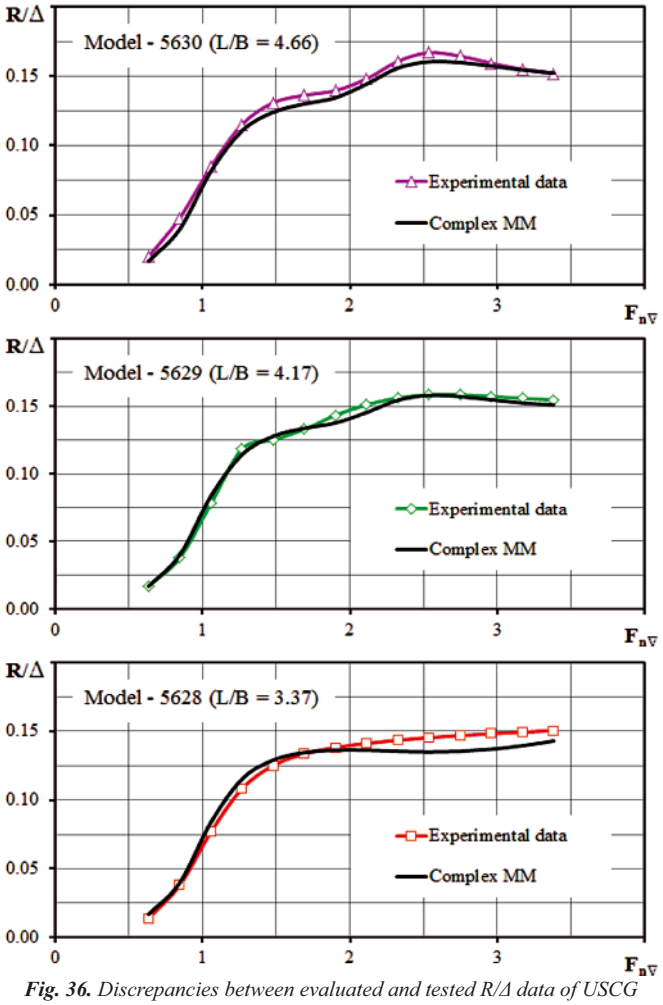

Fig. 36. Discrepancies between evaluated and tested R/Δ data of USCG models 5630, 5629 and 5628

VERIFICATION OF THE MATHEMATICAL MODELS

The goodness of fit of both Simple and Complex mathematical models will be demonstrated for two planing hull models:

- TMB Model No. 4876 (SNAME Small Craft Data Sheet No. 14)
- TUNS Model 3018 (loading cases which were excluded from the database).

TMB Model No. 4876 represents Ray Hunt's deep-V design of 52 ft LCSR (Landing Craft Swimmer Reconnaissance) and has chine and spray strips, as shown is Fig. 37. Calm-water test-data for resistance is given for a model of 3.25 ft, weighting 11.26 lb (see Figure 38). This figure also shows R/Δ evaluated using the Simple and Complex math models (evaluated for LCSR input parameters and scaled down to the same test conditions). Discrepancies are relatively small, and are smaller for the Simple model than for the Complex one, which is unexpected. The discrepancies, however, may be explained: LCSR's spray strips separate the flow, and hence reduce the high speed resistance of deep-V hulls, whereas the math model does not include the effects of bottom spray strips.

For TUNS model No. 3018 (L/B = 3 and β = 18, Figure 3) two loading cases were evaluated, both for L/V$^{1/3}$ = 5.146, but for LCG/L = 0.329 and 0.274, Figs. 39 and 40 respectively. The same figures also show the evaluated values for R/Δ (for model size of L$_{OA}$ = 0.69 m and Δ = 1.825 kg). Note that the

simple math model gave the same results for both positions of LCG, as is f(L/V$^{1/3}$) only. The Complex model, however, clearly depicts the resistance hump (Figure 40) due to LCG position closer to the transom, which is not the case with the Simple model. This also shows the advantage of the Complex math model compared to the Simple one (which is supposed to give relatively good results only if the input parameters are within the average values). Obviously, these two math models are not always equally representative with the experimental data.

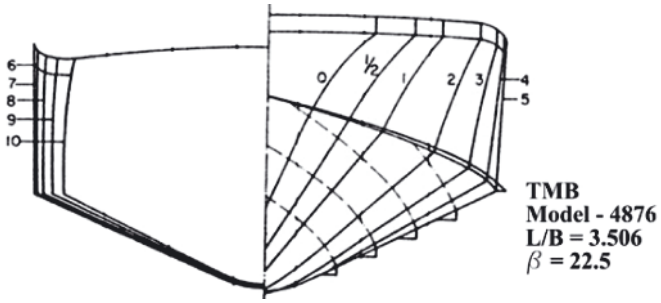

Fig. 37. Body plan of deep-V 52 ft LCSR (TMB Model No. 4876)

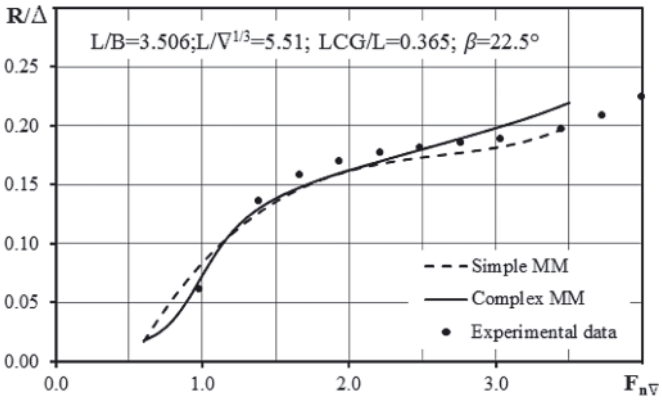

Fig. 38. Discrepancies between evaluated and tested R/Δ data of TMB Model No. 4876

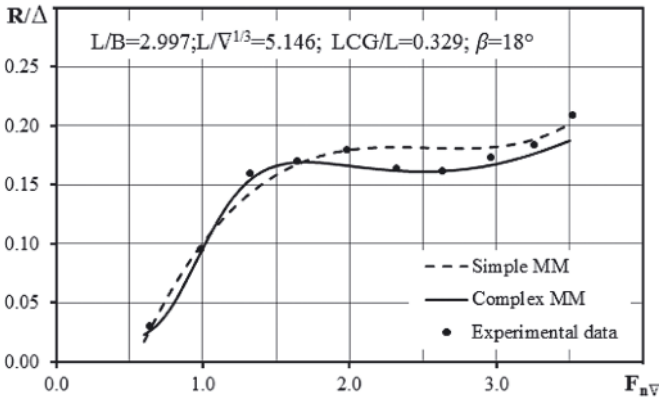

Fig. 39. Discrepancies between evaluated and tested R/Δ data of TUNS model No. 3018

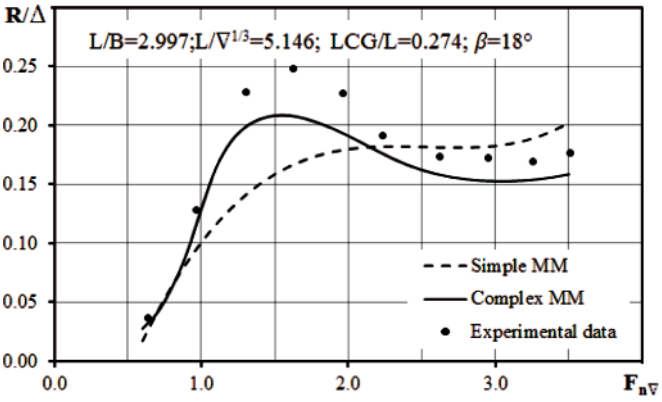

Fig. 40. Discrepancies between evaluated and tested R/Δ data of TUNS model No. 3018

Both mathematical models were examined for several test cases of models belonging to the systematic series and having arbitrary planing hull forms. Verification raised new questions and doubts regarding the quality of the benchmarks. Namely, test cases are often unreliable as are based on small models, see for instance Moore and Hawkins 1969 and Tanaka et al 1991. This subject is beyond the scope of this paper but merits future research.

CONCLUDING REMARKS

For evaluation of calm-water resistance (R/Δ for standard displacement of Δ = 100000 lb) two speed dependent mathematical models, Simple and Complex, were derived. Mathematical models for evaluation of the wetted area (S/V$^{2/3}$) and the length of wetted area (L_K/L) were also derived (since they are needed for resistance evaluations when Δ ≠ 100000 lb). In addition to the volume Froude number (F_{nV}), it is the slenderness ratio which is only used as the independent variable in the Simple model. In the Complex model, the slenderness ratio (L/V$^{1.3}$), the length to beam ratio (L/B), the longitudinal centre of gravity (LCG/L) and the deadrise angle (β) are used. The Complex mathematical model is hence sensitive to variations of all mentioned independent variables. This is obviously not the case with the Simple model.

The Simple model can be used in the concept design phases, when it is practical and desirable to know the relationship between vessel's length and weight, since other hull form parameters are usually unknown. The Complex model can be (and should be) used with other available planing-hull resistance evaluation models, such as for example, Radojcic (1985), Keuning et al (1993) and Savitsky (1964, 2006 and 2012). The proposed model covers hump speeds corresponding to F_{nV} = 0.6 to 3.5. For higher planing speeds (of above $F_{nV} \approx 3$) the Savitsky model is recommended, unless the curved bow shape becomes wetted at low dynamic trim angles.

The derived math models are based on the well known USCG series, and almost unknown prismatic hull form of TUNS Series, both with wide transom which match the contemporary planing hull forms. Keuning (1993) and Radojcic (1985) resistance predictions are based on narrow transom Series 62 (having β = 12.5 to 30 degrees), and wide transom Series 65-B and narrow transom Series 62 (β = 12.5 to 25 degrees), respectively. The here derived Complex model may be incorporated in other power evaluation routines (numerical towing tank performance predictions) or optimization routines with the aim of obtaining the best dimensions, as for example given in Radojcic (1991). It should be noted that tank testing is rarely used in design of small craft due to the cost of tests relative to the cost of the vessel, hence various numerical towing tank performance predictions are used for all design phases.

Furthermore, it seems that the regression analysis is more convenient than artificial neural network (ANN) for simpler relations/equations. For complex relations with many polynomial terms, the regression analysis requires more time and higher levels of skill which is not so pronounced with ANN. Moreover, the step-by-step procedure and regression analysis allow screening of less significant polynomial terms (resulting with smaller polynomial equation) which is not the case with ANN where the number of terms is defined at the very beginning.

The most significant disadvantage of the derived math models is that, in addition to the USCG Series, they are based on the TUNS Series – which is based on relatively small models – hence for some cases the database used is not reliable. It is believed, however, that both math models have smoothed out the inconsistencies and erroneous measurements. So, in some cases mathematical models might be more reliable than the original data.

Whereas some interesting behaviours were observed when checking the quality of the mathematical model and comparing the evaluated values with the model test data of arbitrary hull forms, it was decided to leave that analysis for future work.

Acknowledgement

Authors gratefully acknowledge help and support provided by the high speed and planing craft guru, Mr. Donald Blount who unselfishly shared his knowledge and 50 years experience. Concerning this paper, he was involved in surfacing representative hull form and loading parameters, the subject which is much more delicate than it seems, as well as in giving several useful comments which improved paper's quality.

REFERENCES

1. Blount D. L., Fox D. L.: *Small Craft Power Prediction*, Marine Technology, Vol. 13, No.1, 1976
2. Blount D.: *Prospects for Hard Chine, Monohull Vessels*, Proceedings of the Second Int. Conf. on Fast Sea Transportation - FAST '93, Yokohama, 1993
3. Clement P. E.: *Analyzing the Stepless Planing Boat*, Int. Shipbuilding Progress, No. 33, 1957
4. Clement P. E., Blount D.: *Resistance Tests of a Systematic Series of Planing Hull Forms*, Trans. SNAME, Vol. 71, 1963
5. Delgado-Saldivar G.: *Experimental Investigation of a New Series of Planing Hulls*, M.Sc. Thesis, Technical University of Nova Scotia, Halifax, Nova Scotia, 1993
6. Garo R., Datla R., Imas L.: *Numerical Simulation of Planing Hull Hydrodynamics*, SNAME's Third Chesapeake Powerboat Symposium, Annapolis, 2012
7. Hubble E. N.: *Resistance of Hard-Chine Stepless Planing Craft with Systematic Variation of Hull Form, Longitudinal Centre of Gravity and Loading*, DTNSRDC R&D Report 4307, 1974
8. Keuning, J. A., Gerritsma, J.: *Resistance Tests of a Series of Planing Hull Forms with 25 Degrees Deadrise Angle*, Int. Shipbuilding Progress, Vol. 29, No. 337, 1982
9. Keuning J. A., Gerritsma J., Terwisga P. F.: *Resistance Tests of a Series Planing Hull Forma With 30o Deadrise Angle, and a Calculation Model Based on This and Similar Systematic Series*, Int. Shipbuilding Progress, Vol. 40, No. 424, 1993
10. Kowalyshyn D. H., Metclaf B.: *A USCG Systematic Series of High Speed Planing Hulls*, Trans. SNAME, Vol. 114, 2006
11. Macpherson D.: *Ten Commandments of Reliable Speed Prediction*, Proceedings of Small Craft Resistance and Propulsion Symposium, Michigan, 1996
12. Miljkovic, Z.: *Systems of Artificial Neural Networks in Production Technologies*, University of Belgrade, Faculty of Mechanical Engineering, Belgrade, ISBN 86-7083-455-3 (in Serbian), 2003
13. Moore W., Hawkins F.: *Planing Boat Scale Effects on Trim and Drag (TMB Series 56)*, NSRDC Technical Note No. 128, 1969
14. Morabito M., Snodgrass J.: *The Use of Small Model Testing and Full Scale Trials in the Design of Motor Yacht*, SNAME's Third Chesapeake Powerboat Symposium, Annapolis, 2012
15. Radojcic D.: *An Approximate Method for Calculation of Resistance and Trim of the Planing Hulls*, Ship Science Report No 23, Faculty of Engineering and Applied Science, University of Southampton, Southampton, 1985
16. Radojcic, D.: *An Engineering Approach to Predicting the Hydrodynamic Performance of Planing Craft Using Computer Techniques*, Trans. RINA, Vol. 133, 1991
17. Radojcic D., Rodic T., Kostic N.: *Resistance and Trim Predictions for the NPL High Speed Round Bilge Displacement Hull Series*, RINA's Int. Conf. on Power, Performance & Operability of Small Craft, Southampton, 1997
18. Rojas R.: *Neural Networks - A Systematic Introduction*, Springer-Velrag, Berlin, 1996
19. Savander B. R., Maki K. J., Land J.: *The Effects of Deadrise Variation on Steady Planing Hull Performance*, SNAME's Second Chesapeake Powerboat Symp., Annapolis, 2010
20. Savitsky D.: *Hydrodynamic Design of Planing Hulls*, Marine Technology, Vol. 1, No. 1, 1964
21. Savitsky D., Delorme M., Datla R.: *Inclusion of Whisper-Spray Drag in Performance Prediction Method for Planing Hulls*, New York Metropolitan Section of SNAME, 2006
22. Savitsky D.: *The Effect of Bottom Warp on the Performance of Planing Hulls*, SNAME's Third Chesapeake Powerboat Symposium, Annapolis, 2012
23. Schleicher D., Bowles B.: *Two Speed Gears*, Professional Boat Builder, No. 80, Dec/Jan, 2003
24. Simic A.: *Energy Efficiency of Inland Self-Propelled Cargo Vessels*, Doctoral dissertation, University of Belgrade, Faculty of Mechanical Engineering, Belgrade (in Serbian), 2012
25. *SNAME Small Craft Data Sheets* – Technical and Research Bulletin
26. Tanaka H., Nakato M., Nakatake K., Ueda T., Araki S.: *Cooperative Resistance Tests with Geosim Models of a High-Speed Semi-displacement Craft*, Journal of SNAJ, Vol. 169, 1991.
27. Taunton D. J., Hudson D. A., Shenoi R. A.: *Characteristics of a Series of High Speed Hard Chine Planing Hulls – Part 1: Performance in Calm Water*, Trans. RINA, Vol. 152, Part B2, 2010
28. Zurek S.: *LabVIEW as a tool for measurements, batch data manipulations and artificial neural network predictions*, National Instruments, Curriculum Paper Contest, Przegląd Elektrotechniczny, Nr 4/2007, 2007.

CONTACT WITH THE AUTHORS

Dejan Radojcic[1)], Ph. D.,
Antonio Zgradic[2)], M. Sc.,
Milan Kalajdzic[1)], M. Sc.,
Aleksandar Simic[1], Ph. D.,
[1)] University of Belgrade,
Faculty of Mechanical Engineering,
Dept. of Naval Architecture,
Belgrade, SERBIA
[2)] NAVAR,
Herceg Novi, MONTENEGRO

APPENDIX 1 – Simple Mathematical Model

$$\frac{R}{\Delta} = A \cdot F_{n\nabla}^{3} + B \cdot F_{n\nabla}^{2} + C \cdot F_{n\nabla} + D$$

$$A = -0.0048694 \cdot \left(\frac{L}{\nabla^{1/3}}\right)^{4} + 0.1057838 \cdot \left(\frac{L}{\nabla^{1/3}}\right)^{3} - 0.8432151 \cdot \left(\frac{L}{\nabla^{1/3}}\right)^{2} + 2.8994541 \cdot \left(\frac{L}{\nabla^{1/3}}\right) - 3.5683179$$

$$B = 0.0301221 \cdot \left(\frac{L}{\nabla^{1/3}}\right)^{4} - 0.6562651 \cdot \left(\frac{L}{\nabla^{1/3}}\right)^{3} + 5.2443776 \cdot \left(\frac{L}{\nabla^{1/3}}\right)^{2} - 18.0560600 \cdot \left(\frac{L}{\nabla^{1/3}}\right) + 22.1656778$$

$$C = -0.0508810 \cdot \left(\frac{L}{\nabla^{1/3}}\right)^{4} + 1.1119496 \cdot \left(\frac{L}{\nabla^{1/3}}\right)^{3} - 8.9006694 \cdot \left(\frac{L}{\nabla^{1/3}}\right)^{2} + 30.6066779 \cdot \left(\frac{L}{\nabla^{1/3}}\right) - 37.2112557$$

$$D = 0.0209140 \cdot \left(\frac{L}{\nabla^{1/3}}\right)^{4} - 0.4573261 \cdot \left(\frac{L}{\nabla^{1/3}}\right)^{3} + 3.6580101 \cdot \left(\frac{L}{\nabla^{1/3}}\right)^{2} - 12.5431467 \cdot \left(\frac{L}{\nabla^{1/3}}\right) + 15.14353$$

$$\frac{S}{\nabla^{2/3}} = A \cdot F_{n\nabla}^{3} + B \cdot F_{n\nabla}^{2} + C \cdot F_{n\nabla} + D$$

$$A = 0.0197989 \cdot \left(\frac{L}{\nabla^{1/3}}\right)^{3} - 0.2876721 \cdot \left(\frac{L}{\nabla^{1/3}}\right)^{2} + 1.3944044 \cdot \left(\frac{L}{\nabla^{1/3}}\right) - 2.1175915$$

$$B = -0.1612880 \cdot \left(\frac{L}{\nabla^{1/3}}\right)^{3} + 2.3295698 \cdot \left(\frac{L}{\nabla^{1/3}}\right)^{2} - 11.3511782 \cdot \left(\frac{L}{\nabla^{1/3}}\right) + 18.0264798$$

$$C = 0.4226973 \cdot \left(\frac{L}{\nabla^{1/3}}\right)^{3} - 6.1030996 \cdot \left(\frac{L}{\nabla^{1/3}}\right)^{2} + 29.8350864 \cdot \left(\frac{L}{\nabla^{1/3}}\right) - 49.7163001$$

$$D = -0.4432887 \cdot \left(\frac{L}{\nabla^{1/3}}\right)^{3} + 6.7794188 \cdot \left(\frac{L}{\nabla^{1/3}}\right)^{2} - 33.1423777 \cdot \left(\frac{L}{\nabla^{1/3}}\right) + 58.8177152$$

$$\frac{L_K}{L} = A \cdot F_{n\nabla}^{3} + B \cdot F_{n\nabla}^{2} + C \cdot F_{n\nabla} + D$$

$$A = 0.0010024 \cdot \left(\frac{L}{\nabla^{1/3}}\right)^{3} - 0.0165489 \cdot \left(\frac{L}{\nabla^{1/3}}\right)^{2} + 0.0910387 \cdot \left(\frac{L}{\nabla^{1/3}}\right) - 0.1630761$$

$$B = -0.0021325 \cdot \left(\frac{L}{\nabla^{1/3}}\right)^{3} + 0.0437025 \cdot \left(\frac{L}{\nabla^{1/3}}\right)^{2} - 0.3171667 \cdot \left(\frac{L}{\nabla^{1/3}}\right) + 0.7839794$$

$$C = -0.0049667 \cdot \left(\frac{L}{\nabla^{1/3}}\right)^{3} + 0.0482171 \cdot \left(\frac{L}{\nabla^{1/3}}\right)^{2} + 0.0626019 \cdot \left(\frac{L}{\nabla^{1/3}}\right) - 1.1483516$$

$$D = -0.0086702 \cdot \left(\frac{L}{\nabla^{1/3}}\right)^{3} + 0.1543888 \cdot \left(\frac{L}{\nabla^{1/3}}\right)^{2} - 0.9891214 \cdot \left(\frac{L}{\nabla^{1/3}}\right) + 3.2719934$$

APPENDIX 2 – Complex Mathematical Model

Boundaries of applicability suitable for programming

No.			No.		
1	$0.27 \le LCG/L < 0.33$	$L/V^{1/3} \ge -6.66667 \cdot LCG/L + 6.1$	10	$0.39 \le LCG/L \le 0.41$	$L/B \ge 45 \cdot LCG/L - 15.05$
2	$0.39 \le LCG/L \le 0.41$	$L/V^{1/3} \ge 65 \cdot LCG/L - 21.45$	11	$0.27 \le LCG/L < 0.36$	$L/B \le 3.5$
3	$0.27 \le LCG/L < 0.33$	$L/V^{1/3} \le 6.66667 \cdot LCG/L + 4.7$	12	$3.5 < L/B \le 4.7$	$LCG/L \ge 0.36$
4	$0.39 \le LCG/L \le 0.41$	$L/V^{1/3} \le -35 \cdot LCG/L + 20.55$	13	$0.35 \le LCG/L \le 0.41$	$\beta \ge 100 \cdot LCG/L - 23$
5	$2.5 \le L/B < 4.0$	$L/V^{1/3} \ge 0.866667 \cdot L/B + 1.73333$	14	$0.39 \le LCG/L \le 0.41$	$\beta \le -150 \cdot LCG/L + 82.5$
6	$4.0 \le L/B \le 4.7$	$L/V^{1/3} \ge 5.2$	15	$12° \le \beta \le 14°$	$L/B \le 3.5$
7	$2.5 \le L/B \le 3.5$	$L/V^{1/3} \le 1.3 \cdot L/B + 2.35$	16	$14° < \beta \le 18°$	$L/B \le 0.3 \cdot \beta - 0.7$
8	$3.5 < L/B \le 4.7$	$L/V^{1/3} \le -0.583333 \cdot L/B + 8.94167$	17	$21° \le \beta \le 24°$	$L/B \le -0.4 \cdot \beta + 13.1$
9	$0.27 \le LCG/L \le 0.35$	$L/B \ge -5 \cdot LCG/L + 4.25$			

Resistance to weight ratio – R/Δ

$$Y = \frac{\operatorname{sig}\left(d_v + \sum_{w=1}^{3}\left(D_{wv} \times \operatorname{sig}\left(c_w + \sum_{i=1}^{5}\left(C_{iw} \times \operatorname{sig}\left(b_i + \sum_{j=1}^{7}\left(B_{ji} \times \operatorname{sig}\left(a_j + \sum_{k=1}^{5}(A_{kj} \times (P_k X_k + R_k))\right)\right)\right)\right)\right)\right) - G}{H}$$

where:
$X_K = \{L/B, L/V^{1/3}, F_{nV}, LCG/L, \beta\}$
$Y = R/\Delta$
G, H, P_k, R_k, A_{kj}, B_{ji}, C_{iw}, D_{wv}, a_j, b_i, c_w, d_v are polynomial coefficients that follow:

J	A_{1j}	A_{2j}	A_{3j}	A_{4j}	A_{5j}	a_j
1	1.7456920	2.7293300	8.8455260	5.4907050	-9.3073300	-9.8579260
2	0.2898082	-3.1160330	20.4518000	-0.8953395	0.0587176	-2.3150330
3	-0.7191356	-3.2455800	2.2043970	1.0204330	1.1992110	-2.7231650
4	0.5621026	2.9209610	8.5967350	1.6920190	0.3731644	-3.5395460
5	-7.5173060	-1.3333580	-0.0657259	-1.0204240	-0.3872136	2.1804750
6	-6.2340650	4.1786120	8.8794550	2.3562540	2.3852490	-7.7696170
7	0.3437763	0.9243057	23.8714800	0.3581851	0.1575263	-2.5768110

I	B_{1i}	B_{2i}	B_{3i}	B_{4i}	B_{5i}	B_{6i}	B_{7i}	b_i
1	-2.4406510	2.1080950	7.6929170	-6.1960370	-5.0275680	3.0244980	10.1942600	-7.8806800
2	-3.0829330	1.8681110	3.5004800	-12.5751600	-1.8650630	3.8124340	13.9847500	-5.2925420
3	0.0122627	-4.3228210	0.4912690	-15.3144400	0.6553449	13.0049100	10.0027600	-4.6389580
4	1.3330090	9.3863860	-2.6382690	-3.5427440	-24.9670200	-0.3168464	1.4468000	-7.8299870
5	1.0186670	-0.2119331	0.1647189	-4.2780550	0.3412170	0.4457378	7.2457090	-4.3010290

W	C_{1w}	C_{2w}	C_{3w}	C_{4w}	C_{5w}	c_w
1	-7.0169640	1.0933530	-5.2393960	0.4377735	-5.5052590	-0.3100626
2	-3.2096000	-3.6988810	-11.5074100	-6.9135450	-6.0141480	11.2548400
3	2.9190180	-9.8329010	0.7894529	-17.4901300	6.3501410	5.8545430

V	D_{1v}	D_{2v}	D_{3v}	d_v
1	-6.9155950	-9.0677310	-0.9125847	10.0196700

	L/B	$L/V^{1/3}$	Fn_V	LCG/L	β
P_k	0.4334425	0.3021148	0.1665957	6.5312046	0.0750000
R_k	-1.0323493	-1.1270393	-0.0434102	-1.7402032	-0.8500000
H	3.1461161				
G	0.0266244				

Wetted area coefficient – $S/V^{2/3}$

$$Y = \frac{\operatorname{sig}\left(b_i + \sum_{j=1}^{2}\left(B_{ji} \cdot \operatorname{sig}\left(a_j + \sum_{k=1}^{4}(A_{kj} \cdot (P_k X_k + R_k))\right)\right)\right) - G}{H}$$

where:
$X_K = \{L/B, F_{nV}, L/V^{1/3}, LCG/L\}$
$Y = R/\nabla^{2/3}$
G, H, P_k, R_k, A_{kj}, B_{ji}, a_j, b_i are polynomial coefficients that follow:

j	A_{1j}	A_{2j}	A_{3j}	A_{4j}	a_j
1	-1.0502660	4.8476660	-1.5388710	-1.5804480	-0.4047123
2	2.0970270	-1.0619980	-3.1135780	-0.3070406	1.6046860

i	B_{1i}	B_{2i}	b_i
1	-2.7913260	-3.2475410	2.4859060

	L/B	Fn_V	$L/V^{1/3}$	LCG/L
P_k	0.4157620	0.2589555	0.3021148	6.9230769
R_k	-0.9881993	-0.0951964	-1.1270393	-1.8476154
H	0.1007964			
G	-0.2070596			

Length of wetted area – L_K/L

$$\frac{L_K}{L} = A \cdot F_{n\nabla}^{3} + B \cdot F_{n\nabla}^{2} + C \cdot F_{n\nabla} + D$$

$$A = -19.861 \cdot \left(\frac{LCG}{L}\right)^3 + 17.895 \cdot \left(\frac{LCG}{L}\right)^2 - 5.0552 \cdot \left(\frac{LCG}{L}\right) + 0.4443$$

$$B = 198.98 \cdot \left(\frac{LCG}{L}\right)^3 - 188.93 \cdot \left(\frac{LCG}{L}\right)^2 + 57.04 \cdot \left(\frac{LCG}{L}\right) - 5.4136$$

$$C = -548.66 \cdot \left(\frac{LCG}{L}\right)^3 + 541.85 \cdot \left(\frac{LCG}{L}\right)^2 - 171.02 \cdot \left(\frac{LCG}{L}\right) + 16.936$$

$$D = 347.6 \cdot \left(\frac{LCG}{L}\right)^3 - 359.66 \cdot \left(\frac{LCG}{L}\right)^2 + 120.79 \cdot \left(\frac{LCG}{L}\right) - 12.097$$